BALLISTIC ENERGY PARAMETER CONTROLLER FOR ATMOSPHERIC REENTRY OF A LIFTING BODY

Dennis Navin

Air Force Institute of Technology
Wright-Patterson Air Force Base, Ohio

June 1973

Unclassified
Security Classification

DOCUMENT CONTROL DATA - R & D

(Security classification of title, body of abstract and indexing annotation must be entered when the overall report is classified)

1. ORIGINATING ACTIVITY (Corporate author)

Air Force Institute of Technology (AFIT-SE)
Wright-Patterson AFB, Ohio 45433

2a. REPORT SECURITY CLASSIFICATION

Unclassified

2b. GROUP

3. REPORT TITLE

Ballistic Energy Parameter Controller for Atmospheric Reentry of a Lifting Body

4. DESCRIPTIVE NOTES (Type of report and inclusive dates)

AFIT Thesis

5. AUTHOR(S) (First name, middle initial, last name)

Dennis (NMI) Navin
1/Lt USAF

6. REPORT DATE	7a. TOTAL NO. OF PAGES	7b. NO. OF REFS
June 1973	69	9

8a. CONTRACT OR GRANT NO.	9a. ORIGINATOR'S REPORT NUMBER(S)
b. PROJECT NO. N/A	GGC/EE/73-11
c.	9b. OTHER REPORT NO(S) (Any other numbers that may be assigned this report)
d.	

10. DISTRIBUTION STATEMENT

This document has been approved for public release and sale; its distribution is unlimited.

11. SUPPLEMENTARY NOTES

Approved for public release; IAW AFR 190-17
JERRY C. HIX, Captain, USAF
Director of Information

12. SPONSORING MILITARY ACTIVITY

Air Force Flight Dynamics Laboratory
Wright-Patterson AFB, Ohio 45433

13. ABSTRACT

A preliminary investigation was conducted on the usefulness of the nondimensional ballistic energy parameter Q in a control scheme for the atmospheric reentry of a lifting body with a maximum L/D of 2. A feasible control scheme was developed that allowed onboard calculation of the angle of attack which was used as the control. The control scheme was used over a wide spread of surface ranges while still meeting criteria on heating rate, deceleration and obtaining a desired final velocity. The final altitude was near that desired.

The control scheme is flexible in that it has the capability of updating itself continually as its states become better known and if the control becomes saturated for a part of the reentry trajectory the scheme will pick up again when the vehicle returns to a controllable state. The development was in two dimensional space and comparisons were made with desireable reference trajectories.

DD FORM 1 NOV 68 1473

ia

Unclassified
Security Classification

14. KEY WORDS	LINK A		LINK B		LIN
	ROLE	WT	ROLE	WT	ROLE
Reentry					
Atmospheric					
Lifting Body					
Nondimensional Ballistic Energy Parameter					
Controller					
Feasible Control					

BALLISTIC ENERGY PARAMETER CONTROLLER FOR ATMOSPHERIC REENTRY OF A LIFTING BODY

THESIS

GGC/EE/73-11

DENNIS NAVIN
1/Lt. USAF

Approved for public release; distribution unlimited.

GGC/EE/73-11

BALLISTIC ENERGY PARAMETER CONTROLLER FOR ATMOSPHERIC REENTRY OF A LIFTING BODY

THESIS

Presented to the Faculty of the School of Engineering of
the Air Force Institute of Technology
Air University
in Partial Fulfillment of the
Requirements for the
Master of Science Degree
in Electrical Engineering

by

Dennis Navin, B.S.E.E.
1/Lt. USAF

Graduate Guidance and Control

June 1973

Approved for public release; distribution unlimited.

ic

Preface

For any manned reentry, of utmost importance is the safety of the crew and their vehicle. In this paper is a preliminary investigation of the usefulness of the nondimensional ballistic parameter Q in a control scheme to bring a lifting body safely through the first two phases of reentry - the initial pullout phase and the maneuvering phase. The vehicle model considered has the aerodynamic coefficients of a Newtonian flat plate with a maximum L/D of 2. Motion is confined to two dimensional space.

A control scheme is developed which allows onboard calculation of angle of attack. Consideration is given to heating rate, total heat, deceleration, and meeting end conditions as criteria for a useful control scheme. The control scheme developed meets these criteria rather well.

A problem which was preliminary to the controller investigation was the generation of optimal and near optimal trajectories for comparison. In this I would like to express my gratitude to Captain David South, my sponsor, for the use of his work. I would also like to thank Major James E. Funk, my thesis advisor, for his timely advise and Lieutenant Melvin L. Nagel for his candid discussions. Finally, I would like to thank my wife for her patience and for typing this thesis.

Dennis Navin

Contents

		Page
Preface		ii
List of Figures		iv
List of Tables		vi
Abstract		vii
I	Introduction	1
	Statement of the Problem	2
	Sub-Problems	3
	Assumptions and Approximations	4
	Criteria	5
	Sequence of Problem Development	6
II	Problem Development	8
	Vehicle Model	8
	State Equations	10
	End Condition for Reentry	13
III	Preliminary Reference Trajectory Generation	15
	South's Reentry Trajectories	15
	Conjugate Gradient	17
IV	Q-Controller and Trajectories	35
	The Q-Controller	36
	Straight Line Q Trajectories	38
	Second Order Q Trajectories	48
V	Conclusions and Recommendations	57
	Conclusions	57
	Recommendations	58
Bibliography		59
Appendix A:	Derivation of Equations of Motion	60
Appendix B:	Conjugate Gradient	65
	Problem Formulation	65
	Algorithm	67
Vita		70

List of Figures

Figure		Page
1	South's Equilibrium Glide Trajectory	24
2	Control Schedule for South's Equilibrium Glide Trajectory	25
3	South's Optimal Reentry Trajectory	26
4	Control Schedule for South's Optimal Trajectory	27
5	Resulting Reentry Trajectory using Conjugate Gradient for 1730 nm Range	28
6	Control Schedule for Trajectory using Conjugate Gradient for 1730 nm Range	29
7	Resulting Reentry Trajectory using Conjugate Gradient for 2755 nm Range	30
8	Control Schedule for Trajectory using Conjugate Gradient for 2755 nm Range	31
9	Reentry Trajectory using a Constant α up to the Peak Heating Rate then Conjugate Gradient for Total Range of 1730 nm	32
10	Control Schedule for Trajectory using a Constant α up to the Peak Heating Rate then Conjugate Gradient for Total Range of 1730 nm	33
11	Reentry Trajectory using the Straight Line Q-Controller over 1730 nm Total Range	42
12	Control Schedule for Trajectory using the Straight Line Q-Controller over 1730 nm Total Range	43
13	Reentry Trajectory using the Straight Line Q-Controller over 2419 nm Total Range	44
14	Control Schedule for Trajectory using the Straight Line Q-Controller over 2419 nm Total Range	45
15	Representation of Optimal Q Trajectory over 1730 nm Total Range as it Approaches a Straight Line	49

List of Figures (Cont.)

Figure		Page
16	ΔQ Trajectory	49
17	Reentry Trajectory using Second Order Approximation to Optimal over 1730 nm Total Range	53
18	Control Schedule from Trajectory using Second Order Approximation to Optimal over 1730 nm Total Range	54
19	Coordinate Systems E, N, and B	60

List of Tables

Table		Page
I	Reentry Trajectories Using Conjugate Gradient	34
II	Terminal Conditions of Straight Line Q Trajectories for Different Surface Ranges	46
III	Effects of Perturbations in Initial Conditions on Final Conditions	47
IV	Comparison of Control Schemes Used	56

Abstract

A preliminary investigation was conducted on the usefulness of the nondimensional ballistic energy parameter Q in a control scheme for the atmospheric reentry of a lifting body with a maximum L/D of 2. A feasible control scheme was developed that allowed onboard calculation of the angle of attack which was used as the control. The control scheme was used over a wide spread of surface ranges while still meeting criteria on heating rate, deceleration and obtaining a desired final velocity. The final altitude was near that desired.

The control scheme is flexible in that it has the capability of updating itself continually as its states become better known and if the control becomes saturated for a part of the reentry trajectory the scheme will pick up again when the vehicle returns to a controllable state. The development was in two dimensional space and comparisons were made with desireable reference trajectories.

BALLISTIC ENERGY PARAMETER CONTROLLER FOR ATMOSPHERIC REENTRY OF A LIFTING BODY

I Introduction

Research in the field of reentry vehicles for future space operations indicates that the type of vehicle to be used is the lifting body. This class of vehicle allows good maneuverability for economical recovery while maintaining structural integrity under the structural stress and atmospheric heating encountered during reentry.

Reentry of a lifting body into the earth's atmosphere can be divided into four phases. First is the initial pull-out phase where the heating and deceleration of the vehicle are kept to a minimum while allowing the vehicle to be captured by the atmosphere. The second phase is the maneuvering phase at hypersonic speeds where the angle of attack is high to provide in-plane and crossrange maneuverability, low deceleration, and low heating rate. Third is a transistion phase which has as its principal requirement of providing a continuous link between the hypersonic entry and the last phase, subsonic cruise. At subsonic cruise the vehicle will be maneuvered as an aircraft to a landing.

For any manned reentry, the problem of prime interest is the safety of the crew and it is for this reason that

the first and second phases of reentry are the topics of concern for this paper. It is in these phases that deceleration and heating rate can become the most dangerous to the crew and vehicle. So it is the problem of any reentry to reduce the kinetic and potential energy of the vehicle in such a manner as to preserve the structural integrity of the vehicle and the health of the crew. It is this fact that led to the topic of this theses.

Statement of the Problem

The problem considered is the investigation of the non-dimensional parameter Q in a controller for a lifting body reentry vehicle. This parameter, as used in this study, does not have the usual meaning accorded it in the literature on reentry, i.e., total heat. Instead, Q will be the non-dimensional energy term used in the literature on ballistic missile trajectories. It is defined as the squared ratio of the speed of the vehicle, v, to the speed necessary for circular orbit at that altitude, v_{cs}. Since $v_{cs} = \sqrt{\mu/R}$, then (Ref 1 and 2)

$$Q = v^2 R/\mu \tag{1}$$

where

v = velocity of the vehicle

R = distance of the vehicle from the center of the earth

μ = the earth's gravitational constant

As was mentioned earlier, the kinetic and potential energy of a vehicle entering the earth's atmosphere is to be reduced in such a way as to not endanger either the crew or the vehicle. The non-dimensional parameter Q, as defined above, can be looked upon as a non-dimensional energy parameter incorporating both kinetic energy (velocity) and potential energy (altitude). Looking at Q in this manner it was hoped that the way in which it behaved for a well controlled, if not optimal, trajectory would be of such a nature as to be a useful parameter in a controller for reentry.

Sub-Problems

In order to arrive at a desired schedule for Q during reentry, it was necessary to first obtain desired reentry trajectories. Two types of optimal trajectories were considered. The first was obtained using the conjugate gradient optimization scheme as described in Appendix B. For this technique fixed initial conditions were used but only the altitude and velocity were constrained at the terminal range. The cost function consisted of the integral of heating rate with the terminal constraints added as penalties.

The second type of optimal trajectory considered was the result of work currently being done by Capt. David South, a doctoral student at AFIT (Ref 9). His trajectories resulted from the use of the variation of extremals technique (OPQUID) and for this study were used only as examples of well controlled reentry trajectories. Initial and terminal

conditions were fixed for this method as his terminal condition led into an "equilibrium" glide for the first part of the transition phase.

With these nominal trajectories available it was then possible to analyze the schedule for Q, or Q trajectory. It was necessary to manipulate some parts of the Q trajectory to simplify it for use with a controller and still have an approximation to the optimal trajectories. The end result is a simple sub-optimal guidance scheme using the desired Q trajectory to calculate the control (angle of attack) in real time.

Assumptions and Approximations

To make the problem more tractable, several simplifying assumptions were made. The major assumptions are presented here in generalized terms. More detail is brought out in Chapter II. First, the problem was formulated using two-body mechanics assuming the vehicle was close enough to the earth to ignore any perturbations due to either the sun or the moon. Then the earth and its atmosphere were considered to be spherically symmetrical. The atmospheric density was approximated by an exponential (Ref 3). All of these approximations are common practice in reentry studies and do not affect the major characteristics of the results to any great extent.

The equations of motion were confined to two dimensions (in-plane motion) and this does affect the results somewhat

in that it eliminates the possibility of using lateral maneuvers through roll control of the lift vector for cross range corrections and deceleration control. However, a two-dimensional study is sufficient in determining the feasibility of using Q as a controller during reentry and using angle of attack for control.

Another approximation was that of the aerodynamic model for the vehicle. A flat plate drag polar was assumed to simulate the lifting body (Ref 8). This avoids the complication of using one proposed vehicle while ignoring others and is general enough to allow a meaningful study to be completed.

Criteria

It was not desired that the guidance scheme evolved using the Q-controller would be as good as the optimal trajectories. Indeed, if optimizing techniques were used to arrive at these trajectories, then only the exact same control could do as well. The criteria used to judge the usefulness of the Q-controller was that it kept the maximum heating rate below a certain bound and the deceleration well below the tolerance for man. Specifics on these criteria are given later in this report.

Also the Q-Controller must be simple enough to allow real time calculation of control. At the same time it has to allow for variations in initial conditions and still arrive at the desired terminal conditions. This is most

important since the vehicle could be off from the planned trajectory.

It was assumed that all along the trajectory the velocity, altitude, flight path angle, and angle of attack were measurable. This was necessary to calculate Q and also the control once Q had been determined.

Sequence of Problem Development

At the outset of the investigation several fundamental conditions and mathematical models had to be clearly defined to be used throughout the study. This is done in Chapter II and Appendix A. Appendix A contains the derivation of the two-body, two-dimensional equations of motion using the general forces of lift, drag and gravity acting on a point mass.

In Chapter II the math model of the vehicle to be used in the study is defined and incorporated into the equations of motion. With the atmosphere density defined, the system equations are ready for integration.

The initial conditions are chosen for a typical orbital return trajectory from 200 nautical mile orbit with reentry beginning at 400,000 feet. The flight depression angle is 1.738 degrees and the velocity is 24,850 ft/sec. The final conditions to be met are that the altitude be 150,000 feet and velocity between 3,000 and 5,000 ft/sec. These terminal conditions of the initial entry phase coincide with the initial conditions for the transition phase. (Ref 7)

With the problem so formulated, the conjugate gradient is then used to produce near optimal trajectories from which Q-trajectories can be studied. The results from the use of the conjugate gradient technique are presented in Chapter III along with some results from the work done by Capt. South (Ref 9). However, Capt. South's work was done with somewhat different objectives and his results are used only for comparison of the Q variable behavior.

In Chapter IV several methods for approximating the Q-trajectories arrived at in Chapter III are explored. A method for real time calculation of control using straight line approximations is derived and a second order approximation is attempted. The results of these methods are presented and compared in Chapter IV.

II Problem Development

Vehicle Model

The equations of motion for a point mass in two-dimensional space, acted upon by the forces of lift, drag, and gravity, are derived in Appendix A. The vehicle model used in this study to produce the forces of lift and drag has the aerodynamic coefficients of a Newtonian-Flat-Plate drag polar (Ref 8):

$$CL = 1.82 \sin \alpha \cos \alpha |\sin \alpha| \tag{2}$$

$$CD = 0.042 + 1.46 |\sin^3 \alpha| \tag{3}$$

CL is the lift coefficient, CD is the drag coefficient and α is the angle of attack. Using these definitions of parameters CL and CD gives a vehicle model with a maximum lift-over-drag of 2 at an angle of attack of approximately 21 degrees.

The model for the atmospheric density, ρ, as mentioned in the introduction, is an exponential approximation (Ref 3):

$$\rho = \rho_o e^{-\beta h} \tag{4}$$

where

$$\rho_o = 0.0026703 \text{ slugs/ft}^3 \tag{5}$$

$$\beta = 0.425211877 \ (10)^{-4}/\text{ft} \tag{6}$$

and h is the altitude of the vehicle.

Introducing Equations (2), (3), and (4) into the general equations for lift and drag, and dividing by the mass of the vehicle results in the specific force equations for lift and drag:

$$L = C_L(\tfrac{1}{2}\rho v^2)(l^2/m)$$

$$= 1.82 \sin\alpha \cos\alpha |\sin\alpha| (\tfrac{1}{2}\rho_o e^{-\beta h} v^2)(l^2/m) \quad (7)$$

and

$$D = C_D(\tfrac{1}{2}\rho v^2)(l^2/m)$$

$$= (0.042 + 1.46|\sin^3\alpha|)(\tfrac{1}{2}\rho_o e^{-\beta h} v^2)(l^2/m) \quad (8)$$

where v is the magnitude of the velocity of the vehicle, l^2 is the characteristic area of the vehicle, and m is the mass of the vehicle. The term l^2/m was defined as a constant (Ref 8):

$$l^2/m = 1.1907 \text{ ft}^2/\text{slug} \quad (9)$$

The heating rate, q, of the vehicle model is proportional to the cube of the total velocity of the vehicle multiplied by the square root of the atmospheric density. The constant of proportionality for this model, C_h, equals $2(10)^{-8}$ when used with British units and results in Btu/ft^2 sec, i.e., the heating rate with respect to time is

$$q = C_h \rho^{\frac{1}{2}} v^3 \quad (10)$$

Heating rate and its integral, total heat, were used in this study to evaluate the effectiveness of the control schemes

used for the reentry problem. It was desired to keep the maximum heating rate below 100 Btu/ft^2 sec. Of course, the lower the maximum heat rate, the better the control scheme. The total heat was not given any bound as its value depends a great deal on the time of flight. However, it was used as a relative measure of effectiveness for the different control schemes used for a fixed range and fixed end conditions.

State Equations

Inserting Equations (7) and (8) into the general equations of motion derived in Appendix A gives

$$\dot{h} = -v \sin \delta \tag{11}$$

$$\dot{v} = \frac{\mu \sin \delta}{(h+R_o)^2} - \tfrac{1}{2}CD\, \rho_o\, e^{-\beta h}\, v^2 \quad (l^2/m) \tag{12}$$

$$\dot{\delta} = \frac{-v \cos \delta}{h+R_o} + \frac{\mu \cos \delta}{(h+R_o)^2 v} - \tfrac{1}{2}CL\, \rho_o\, e^{-\beta h}\, v \quad (l^2/m) \tag{13}$$

$$\dot{S} = \frac{R_o\, v \cos \delta}{h+R_o} \tag{14}$$

where S is surface range.

Since it was highly unlikely that the surface range would do anything but monotonically increase during the phases of reentry being considered in this study, it was

decided to use the surface range as the independent variable instead of time. This not only eliminates one of state equations but also allows a fixed terminal value for the independent variable to be specified in the optimization problem formulation. This is accomplished by dividing Equations (11), (12), and (13) by Equation (14) to give the remaining states derivatives with respect to surface range:

$$\frac{dh}{dS} = \frac{-(h+R_e)\tan\delta}{R_e} \tag{15}$$

$$\frac{dv}{dS} = \frac{\mu\tan\delta}{(h+R_e)vR_e} - \frac{CD(h+R_e)\rho_e e^{-\beta h} v\,(l^2/2m)}{R_e\cos\delta} \tag{16}$$

$$\frac{d\delta}{dS} = \frac{-1}{R_e} + \frac{\mu}{R_e v^2 (h+R_e)} - \frac{CL\,(h+R_e)\rho_e e^{-\beta h}\,(l^2/2m)}{R_e\cos\delta} \tag{17}$$

It was also desirous to have Q as one of the states and a second set of states which includes Q was developed. Recalling

$$Q = \frac{v^2 R}{\mu} \tag{1}$$

where R is equal to altitude, h, plus the radius of earth, R_e, it would be easiest to replace h with Q as a state of the system. This was done by taking the derivative of (1) with respect to range and making use of Equations (15) and (16).

Then

$$\frac{dQ}{dS} = \frac{2 \tan \delta}{R_o} - \frac{CD\ (h+R_o)^2\ \rho_o\ e^{-\beta h}\ v^2\ (l^2/m)}{\mu\ R_o \cos \delta} - \frac{v^2\ (h+R_o) \sin \delta}{\mu\ R_o \cos \delta} \tag{18}$$

where

$$h = \frac{\mu\ Q}{v^2} - R_o \tag{19}$$

Equation (19) was substituted into (16), (17), and (18) to give the state equations as used with the controllers developed in Chapter IV:

$$\frac{dQ}{dS} = \frac{\tan \delta\ (2-Q)}{R_o} - \frac{CD\ \mu\ Q^2\ \rho_o\ e^{-\beta(\frac{\mu Q}{v^2}-R_o)}\ (l^2/m)}{v^2\ R_o \cos \delta} \tag{20}$$

$$\frac{dv}{dS} = \frac{v \tan \delta}{Q\ R_o} - \frac{\frac{1}{2}CD\ \mu\ Q\ \rho_o\ e^{-\beta(\frac{\mu Q}{v^2}-R_o)}\ (l^2/m)}{v\ R_o \cos \delta} \tag{21}$$

$$\frac{d\delta}{dS} = \frac{-1}{R_o} + \frac{1}{Q\ R_o} - \frac{\frac{1}{2}CL\ \mu\ Q\ \rho_o\ e^{-\beta(\frac{\mu Q}{v^2}-R_o)}\ (l^2/m)}{v^2\ R_o \cos \delta} \tag{22}$$

The heating rate was also divided by the time derivative of surface range so that q could be integrated along with the state equations using surface range as the independent variable:

$$q_s = \frac{\mu C_h \rho^{\frac{1}{2}} Q}{R_e \cos \delta} \qquad (23)$$

where use of the equation for h, (19), was made to eliminate h.

End Condition for Reentry

The initial conditions for the reentry trajectory were stated in the introduction but will be repeated here for continuity in the problem development. The initial conditions for the state equations were

$$h_o = 399{,}263 \text{ ft} \qquad (24)$$

$$v_o = 24{,}850 \text{ ft/sec} \qquad (25)$$

therefore $Q_o = 0.93557$ (26)

and $\delta_o = 1.7377$ deg (27)

The initial value for the independent variable, surface range, was zero, i.e., the earth centered inertial reference frame used in the derivation of the equations of motion in Appendix A was assumed to have its x-axis in the direction where the vehicle enters the atmosphere at 399,263 ft. Also the total heat was assumed to have been negligible up to this point and was set equal to zero.

Different terminal conditions were used depending on the control scheme being used and for making evaluations of guidance schemes. For the conjugate gradient optimization problem the state equations as given in (15), (16), and (17) were

used and the only constraints put on the states at the final range was that the altitude would be 150,000 feet and velocity 4,000 ft/sec. As it turned out the velocity was usually well within the bounds desired and was constrained only as a check on its effect on the Q trajectory which was negligible or to make more detailed comparisons with Q controlled trajectories. The final range was varied to make comparisons with Q controlled trajectories since one desired end result was that there would be some degree of freedom in choosing a final range at the initial entry point of 399,263 feet and still be able to meet other desired end conditions.

For the Q controlled trajectories the state equations as given by (20), (21), and (22) were used. The only constraint on the final states for these trajectories was the final value of Q, Q_f. Since Q is a function of altitude and velocity, using a fixed Q_f does not guarantee final values for either h or v. It was found that the effect is more pronounced on altitude which varied considerably with total range covered by the trajectory. As is implied by this last statement various final ranges were used for the Q controlled trajectories to determine the useful range of the controller.

III Preliminary Reference Trajectory Generation

South's Reentry Trajectories

Before any characteristics of a desired Q trajectory could be ascertained it was necessary to first produce trajectories that were at least near optimal. Two sources were considered. First was the results of work done by Capt. South (Ref 9). Through him were obtained two trajectories - one an "equilibrium" glide and the other an optimum trajectory leading to "equilibrium" conditions at 200,000 feet. The first was used by South to generate end conditions close enough to optimal to permit a Newton-Raphson iteration scheme to converge to the desired initial conditions at 400,000 feet. The vehicle model used by South had a maximum L/D of 1.5 at an angle of attack of 22.15 degrees.

The "equilibrium" glide trajectory can be divided into three distinct parts in terms of control. The first part is a constant angle of attack, 55 degrees, until the flight path depression angle, δ, becomes negative wherein the second part begins. This is the pullout phase and uses for a control law

$$\ddot{h} + 2\sqrt{k}\,\dot{h} + k\,(h - 250{,}000) = 0 \qquad (28)$$

or

$$\ddot{h} + 2\zeta\omega_n\,\dot{h} + \omega_n^2\,(h - 250{,}000) = 0 \qquad (29)$$

where

$$k = 10^{-2} \tag{30}$$

which means

$$\omega_n = 0.1 \text{ rad/sec} \tag{31}$$

for

$$\zeta = 1 \tag{32}$$

From Equation (11)

$$\dot{h} = - v \sin \delta \tag{11}$$

which is substituted into (29) and $\ddot{h}$ is solved for. Then the derivative is taken of (11) which gives two equations for $\ddot{h}$. The control is then solved for by iteration. This control law is used until α reaches 54.74 degrees and then α is held constant at this angle for the rest of the flight. That is, the result of this control law being used is a trajectory where the altitude of the vehicle ascends to 250,000 feet after pullout at which it stays until the control law commands an angle of attack of 54.74 degrees. This is the angle of attack for maximum lift for the vehicle model being used and phugoid motion is damped out for the remainder of the trajectory. These results are shown graphically in Figures 1 and 2.

It should be noted here that the initial and final conditions for the trajectories resulting from Capt. South's work were not the same as stated previously in this paper,

his trajectories were used only for observing the behavior of the parameter Q during a well controlled reentry. The initial conditions for South's trajectories were

$$h = 400{,}000 \text{ ft} \tag{33}$$

$$v = 25850 \text{ ft/sec} \tag{34}$$

$$\delta = 2.159 \text{ deg} \tag{35}$$

The values of velocity and the flight depression angle from the equilibrium glide trajectory at 200,000 feet were used as terminal conditions to start the Newton-Raphson iterations which converged to the desired initial conditions and the resulting optimal trajectory is presented in Figures 3 and 4. Note that the end conditions for this optimal trajectory meet the conditions for a glide trajectory with phugoid motion damped out for the remainder of the flight.

The analysis of these trajectories as they apply to the Q-controller will be presented later.

Conjugate Gradient

The second source for optimal reentry trajectories was the conjugate gradient optimization scheme. The general equations and algorithm for this method are presented in Appendix B. The more specific equations are presented here.

The state equations for the conjugate gradient problem formulation were those as shown on page 11, Equations (15), (16), and (17), and the initial conditions were those given

on page 13, Equations (24) through (27). To complete the problem formulation a cost function which reflected the most desireable qualities for a reentry trajectory was needed. The squared integral of the heating rate was chosen since it was desired to preserve the vehicles structural reliability and since also the deceleration schedule for a reentry vehicle very nearly parallels the heating rate schedule. Then penalty functions were added to this cost function to constrain the terminal values of altitude, h, and velocity, v.

Then the total cost function in Meyer form was

$$J = CK^2(S_f) + D\left[h(S_f) - 150000\right]^2 + E\left[v(S_f) - 4000\right]^2 \qquad (36)$$

where

$$K(S_f) = \int_o^{S_f} q_s \, dS \qquad (37)$$

and C, D, and E were weighting factors. Also S_f was the desired final range and q_s was as defined in Equation 23, page 13. For the cost function to be so defined it was necessary to define K as an additional state with its derivative equal to q_s. Ordinarily this extra state, which is the total heat absorbed, would have the symbol Q, but this would lead to confusion in this paper and so the symbol K was adopted for total heat.

The states were defined as

$$\begin{bmatrix} x_1 \\ x_2 \\ x_3 \\ x_4 \end{bmatrix} = \begin{bmatrix} h \\ v \\ \delta \\ K \end{bmatrix} \tag{38}$$

As was mentioned earlier, it was not necessary to use the constraint on velocity so E was usually set equal to zero. Two runs were made where E was not equal to zero and proved not to change the trajectory noticeably.

The procedure as outlined in Appendix B was followed to form the Hamiltonian and the range derivatives of the costates were determined:

$$\frac{d\lambda_1}{dS} = \frac{\lambda_1 \tan x_3}{R_o} + \frac{\lambda_2 \mu \tan x_3}{(x_1+R_o)^2 x_2} + \frac{\lambda_3 \mu}{(x_1+R_o)^2 x_2^2}$$

$$+ \frac{\lambda_2(0.042 + 1.46|\sin^3 \alpha|)\, \rho_o\, e^{-\beta x_1}\, x_2 (l^2/2m)\left[1-\beta(x_1+R_o)\right]}{R_o \cos x_3}$$

$$+ \frac{\lambda_3(1.86 \sin \alpha \cos \alpha |\sin \alpha|)\, \rho_o\, e^{-\beta x_1} (l^2/2m)\left[1-\beta(x_1+R_o)\right]}{R_o \cos x_3}$$

$$- \frac{\lambda_4 C_h x_2^2 \rho_o e^{-\frac{1}{2}\beta x_1} \left[1-\frac{1}{2}\beta(x_1+R_o)\right]}{R_o \cos x_3} \tag{39}$$

$$\frac{d\lambda_2}{dS} = \frac{\mu}{R_o x_2^2 (x_1+R_o)} \left[\lambda_2 \tan x_3 + \frac{2\lambda_3}{x_2}\right]$$

$$+ \frac{\lambda_2(0.042 + 1.46|\sin^3 \alpha|) \rho_o e^{-\beta x} (x_1+R_o)(l^2/2m)}{R_o \cos x_3}$$

$$- \frac{\lambda_4 C_h 2 \rho_o^{\frac{1}{2}} e^{-\frac{1}{2}\beta x_1}(x_1+R_o) x_2}{R_o \cos x_3} \tag{40}$$

$$\frac{d\lambda_3}{dS} = \frac{1}{R_o \cos x_3} \left[\lambda_1 (x_1+R_o) - \frac{\lambda_2 \mu}{(x_1+R_o) x_2}\right]$$

$$+ \frac{\tan x_3 \rho_o e^{-\beta x_1}(l^2/2m)(x_1+R_o)}{R_o \cos x_3}$$

$$\left[\lambda_2(0.42 + 1.46|\sin^3 \alpha|)x_2\right.$$

$$\left. + \lambda_3 1.82 \sin \alpha \cos \alpha |\sin \alpha|\right]$$

$$- \frac{\lambda_4 C_h \rho_o^{\frac{1}{2}} e^{-\frac{1}{2}\beta x_1} x_2^2 \tan x_3 (x_1+R_e)}{R_e \cos x_3} \tag{41}$$

$$\frac{d\lambda_4}{dS} = 0 \tag{42}$$

Then the associated costates for these states at the final range, S_f, were

$$\lambda_i(S_f) = \left.\frac{\partial J}{\partial x_i}\right|_{S_f} \qquad i = 1,\ldots,4 \tag{43}$$

or

$$\begin{bmatrix} \lambda_1(S_f) \\ \lambda_2(S_f) \\ \lambda_3(S_f) \\ \lambda_4(S_f) \end{bmatrix} = \begin{bmatrix} 2D\left[x_1(S_f)-150000\right] \\ 2E\left[x_2(S_f)-4000\right] \\ 0 \\ 2C\ x_4(S_f) \end{bmatrix} \tag{44}$$

The gradient was given by

$$g(\alpha) = \frac{\partial H}{\partial \alpha} \tag{45}$$

but since there were trigonometric functions of α inclosed within absolute value signs these functions were transformed

to trigonometric functions times sgn α where sgn α was treated as a constant. Then the gradient was

$$g(\alpha) = \frac{\text{sgn } \alpha \; \rho_o \; e^{-\beta x_1} \; (l^2/2m)(x_1+R_e)}{R_e \cos x_3}$$

$$\left[- 4.38 \; \lambda_2 \; x_2 \sin^2 \alpha \cos \alpha \right.$$

$$\left. - 1.82 \; \lambda_3 \; (2 \sin \alpha \cos^2 \alpha - \sin^3 \alpha) \right] \tag{46}$$

Equations (36) through (46) were applied, using the algorithm presented in Appendix B, to three reentry conditions. The first two had the initial conditions as given in Equations (24) through (27), page 13, but with different terminal ranges. The third trajectory had the same initial conditions but used a constant angle of attack up to the first peak in heating rate and then conjugate gradient was applied from that point to the terminal conditions. The graphical presentation of these trajectories are shown in Figures 5 through 10.

Since these trajectories have the same initial conditions and vehicle model as was used for the Q controlled trajectories presented later, some of the particulars are presented in Table I. The graphical results of these trajectories are shown in Figures 5 through 10.

As is pointed out in the table the second trajectory did not have a constraint on the final velocity. The final velocity of 3109 ft/sec was within the desired range of velocities desired and since this trajectory was used only for analysis of the Q schedule the final velocity wasn't constrained.

The third trajectory of Table I, Figures 9 and 10, is the result of using a constant angle of attack of 59.961 degrees and then a conjugate gradient determined control schedule from that point where the first peak in heat rate occurs for the constant α trajectory. The angle 59.961 degrees was determined using a straight forward search routine to find the constant α which gave the lowest peak heat rate using the given initial conditions.

The analysis of these trajectories, those given by Capt. South, and the state equation for Q which led to the Q-controller follows next.

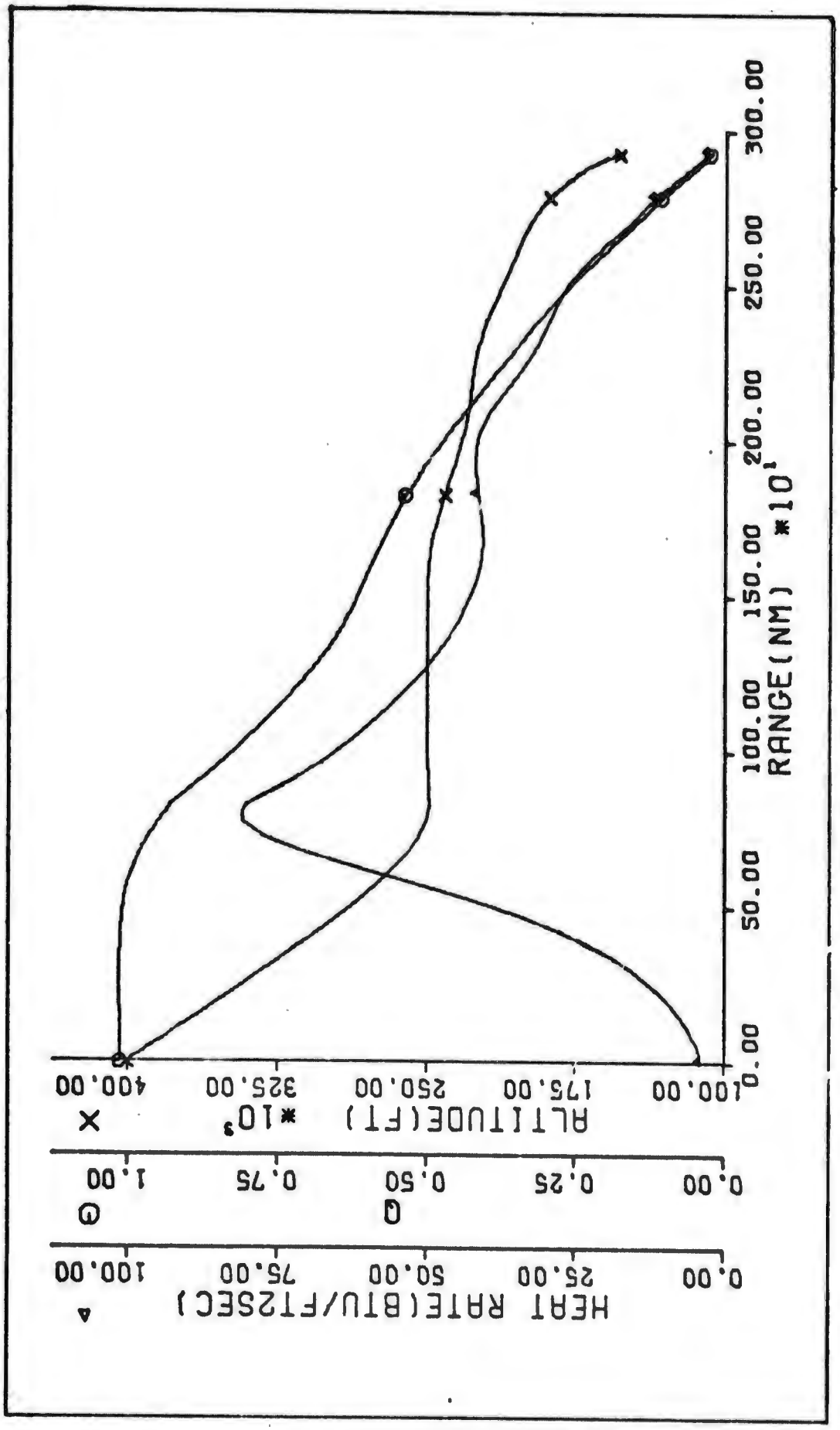

Figure 1. South's Equilibrium Glide Trajectory

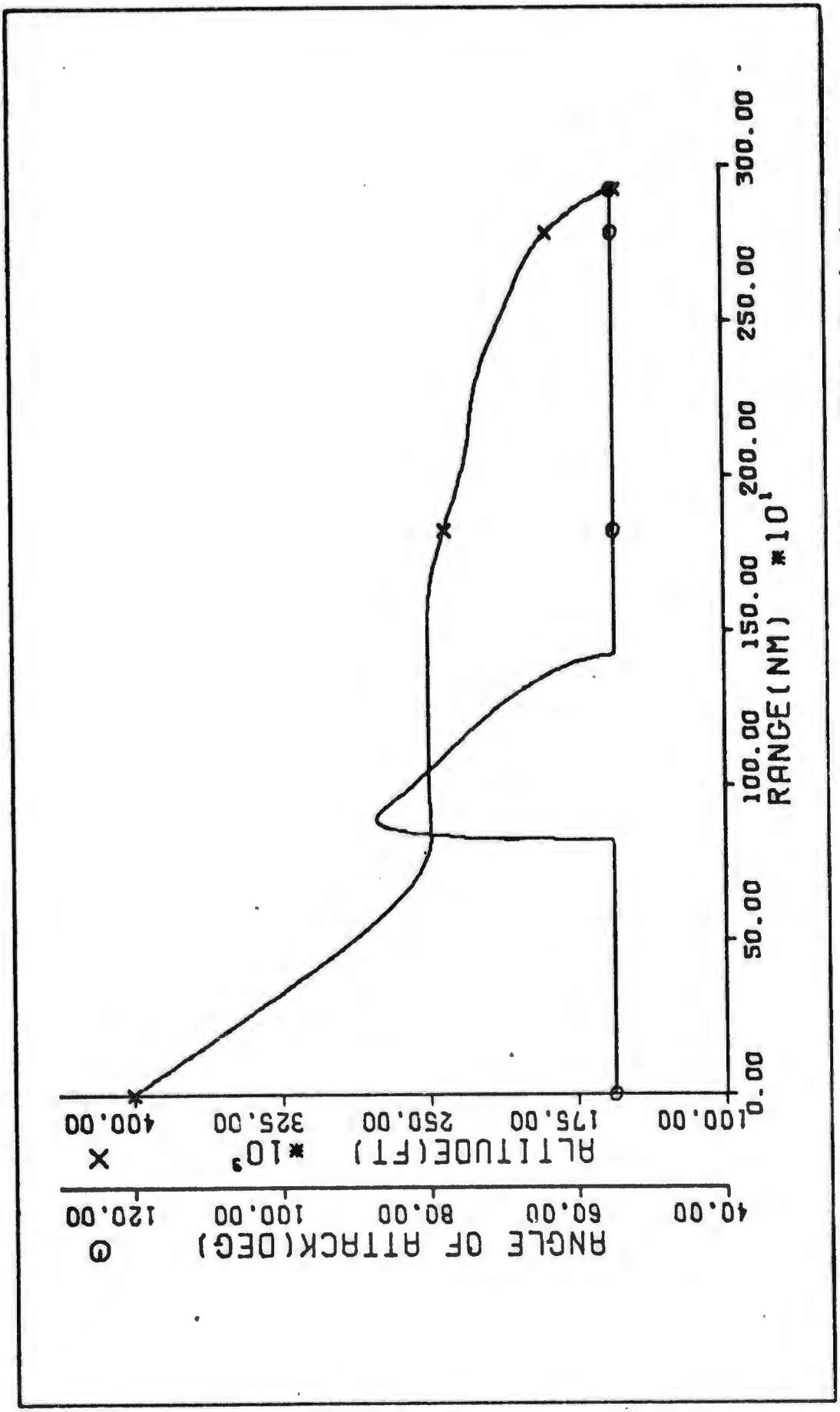

Figure 2. Control Schedule for South's Equilibrium Glide Trajectory

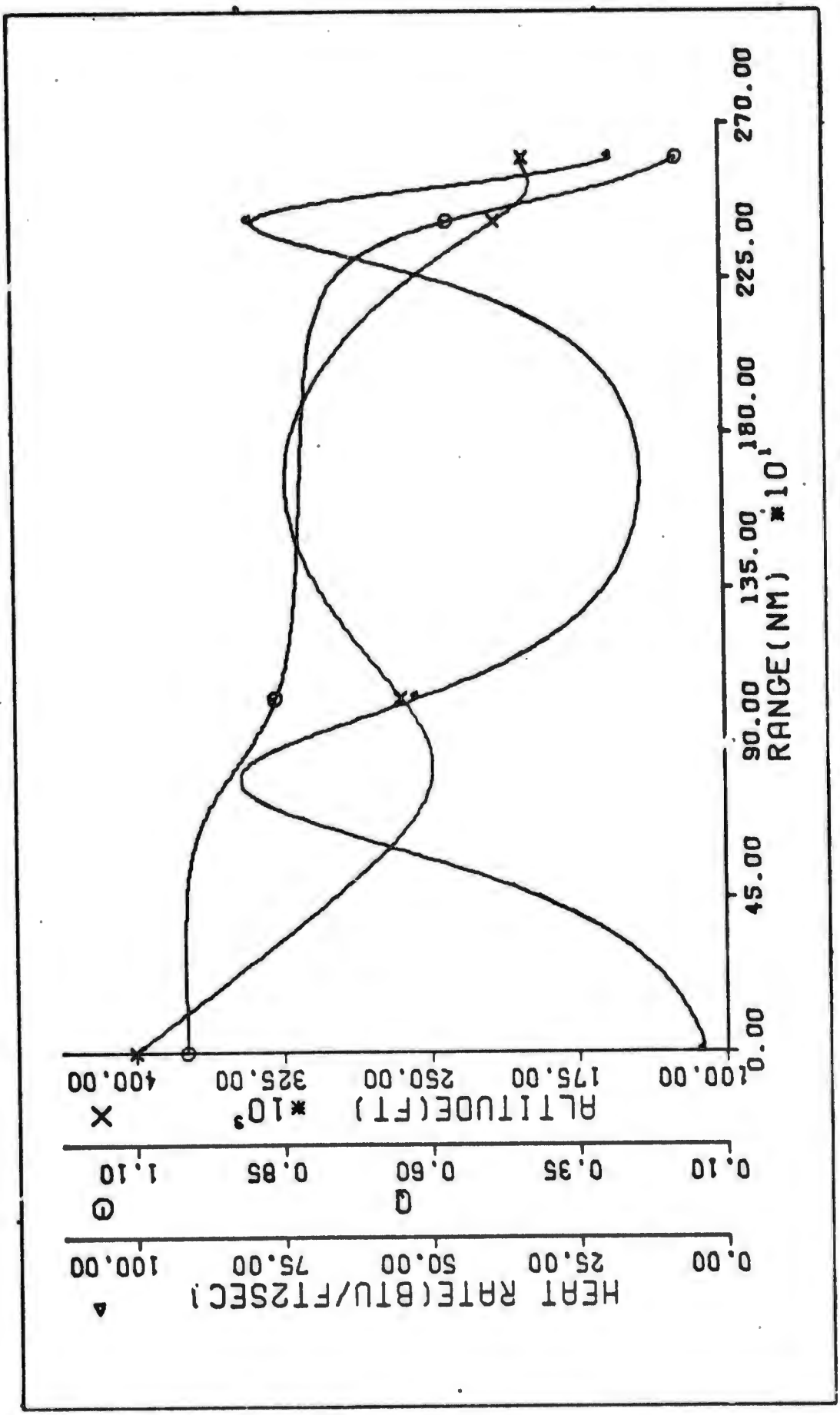

Figure 3. South's Optimal Reentry Trajectory

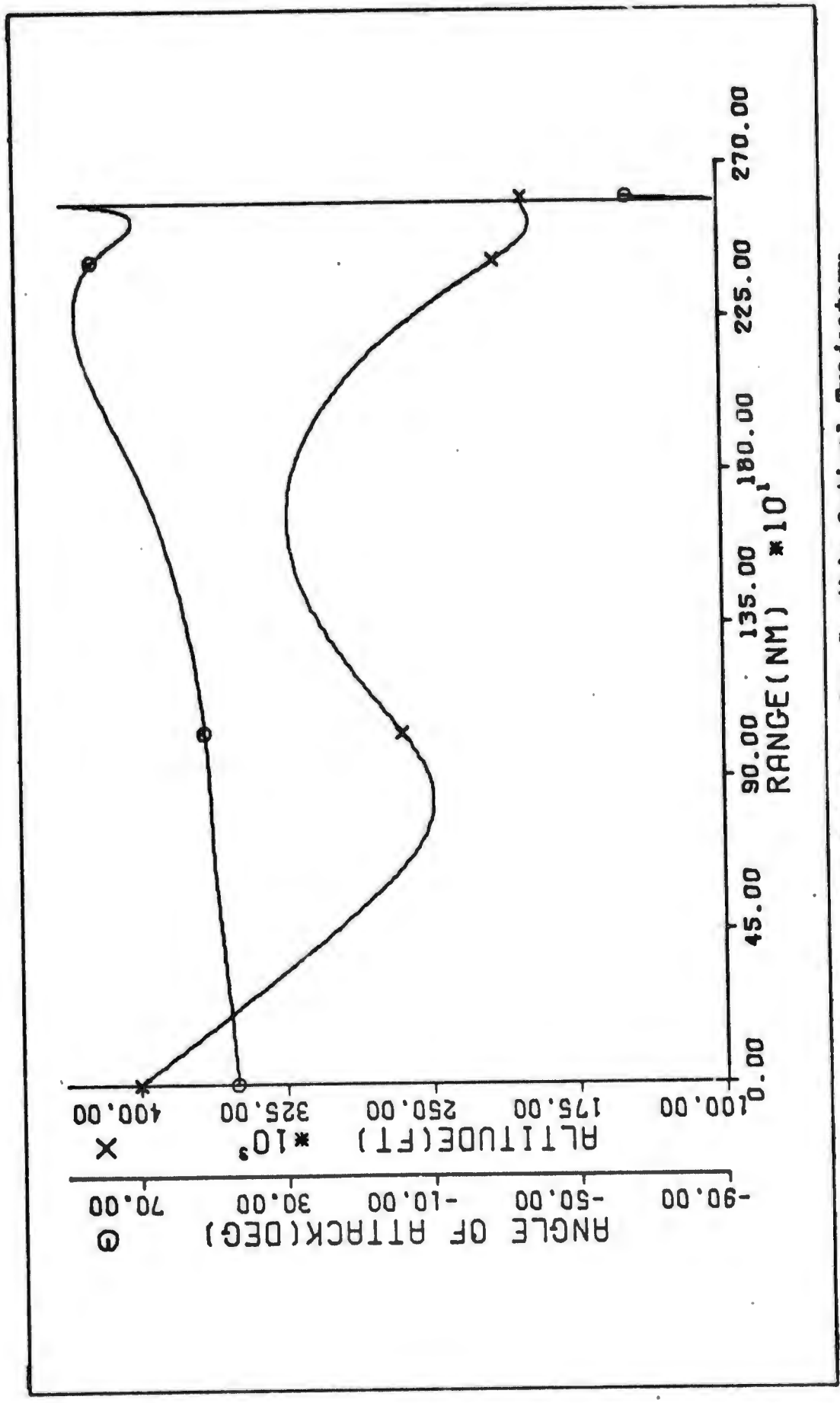

Figure 4. Control Schedule for South's Optimal Trajectory

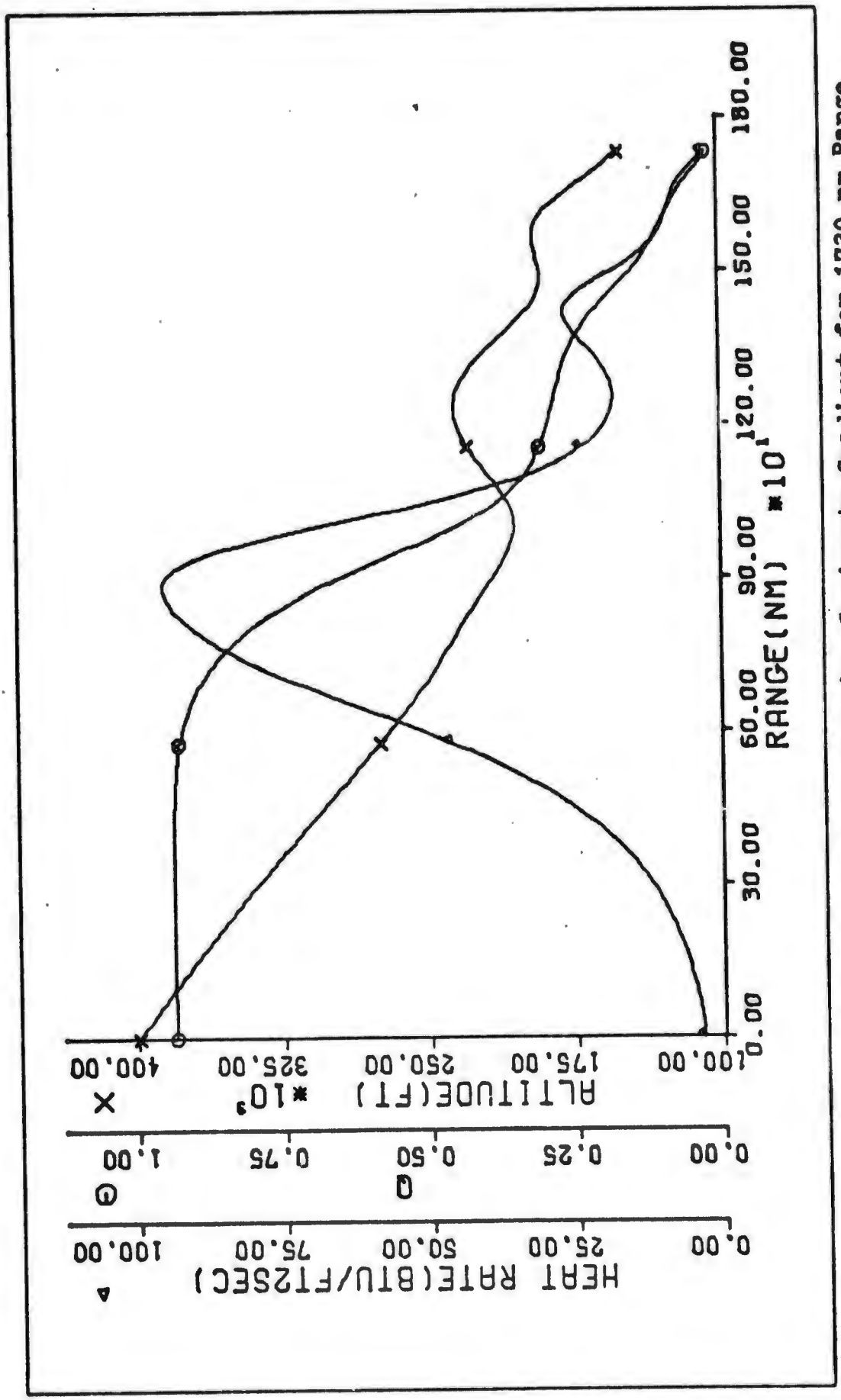

Figure 5. Resulting Reentry Trajectory using Conjugate Gradient for 1730 nm Range

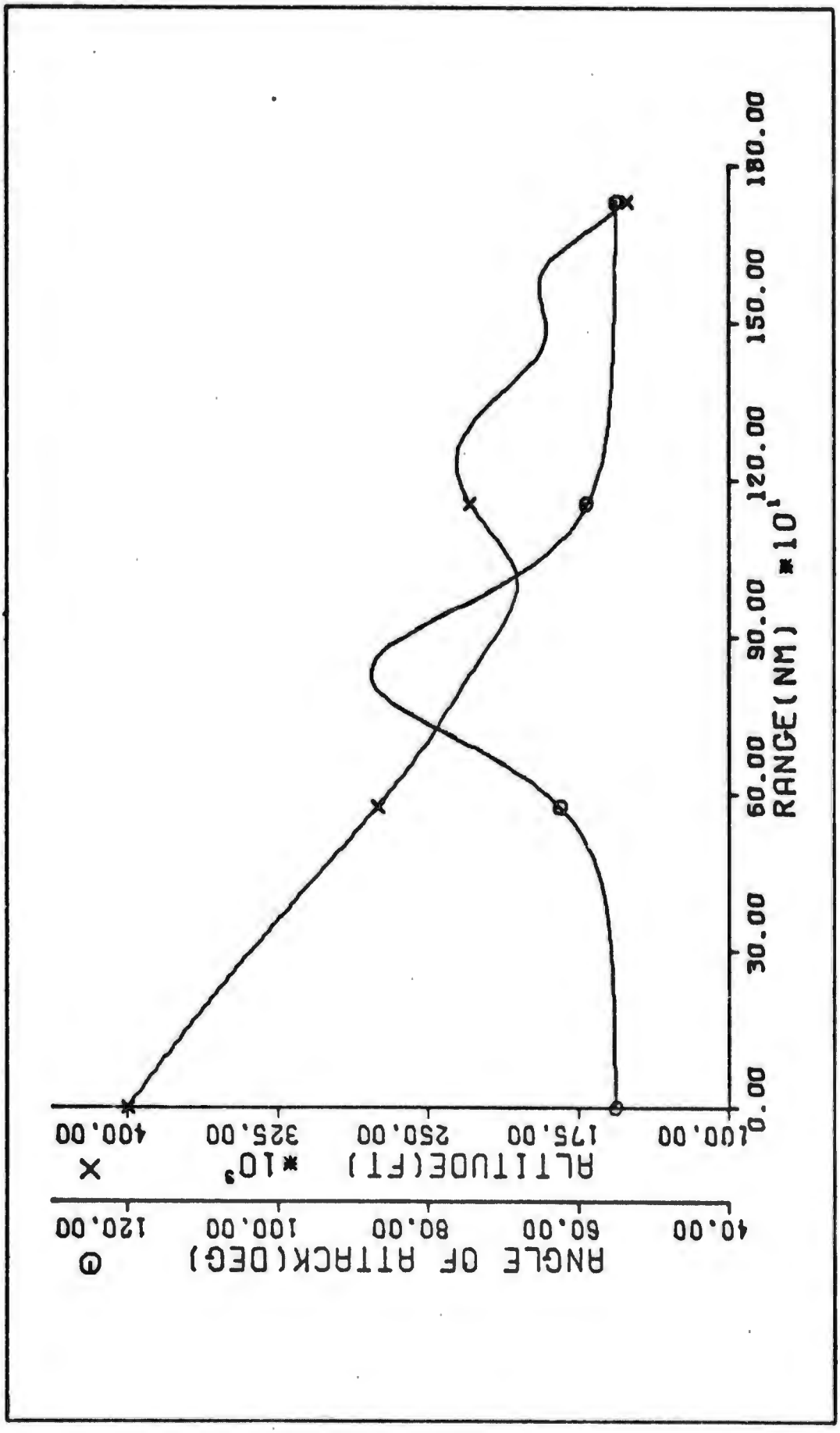

Figure 6. Control Schedule for Trajectory using Conjugate Gradient for 1730 nm Range

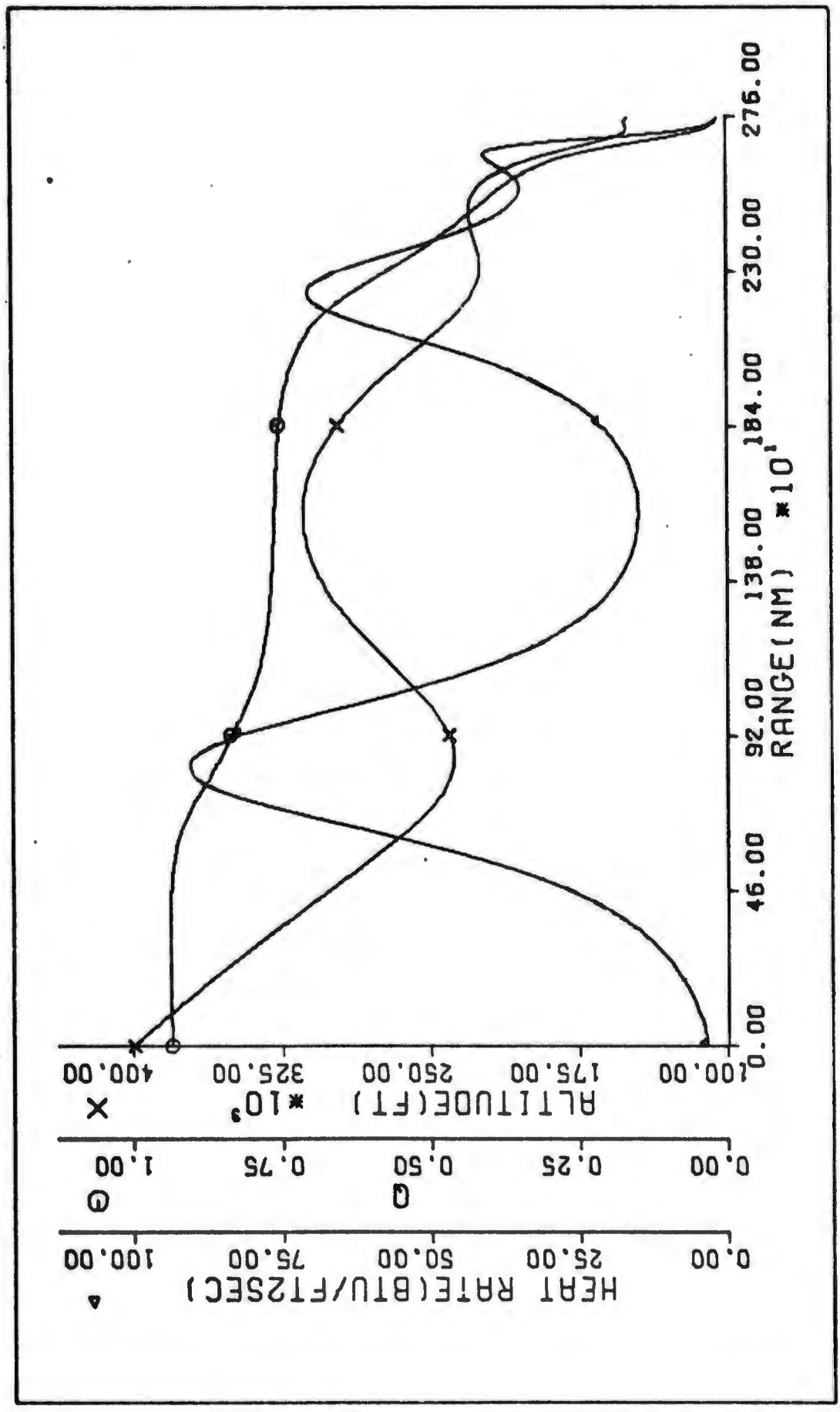

Figure 7. Resulting Reentry Trajectory using Conjugate Gradient for 2755 nm Range

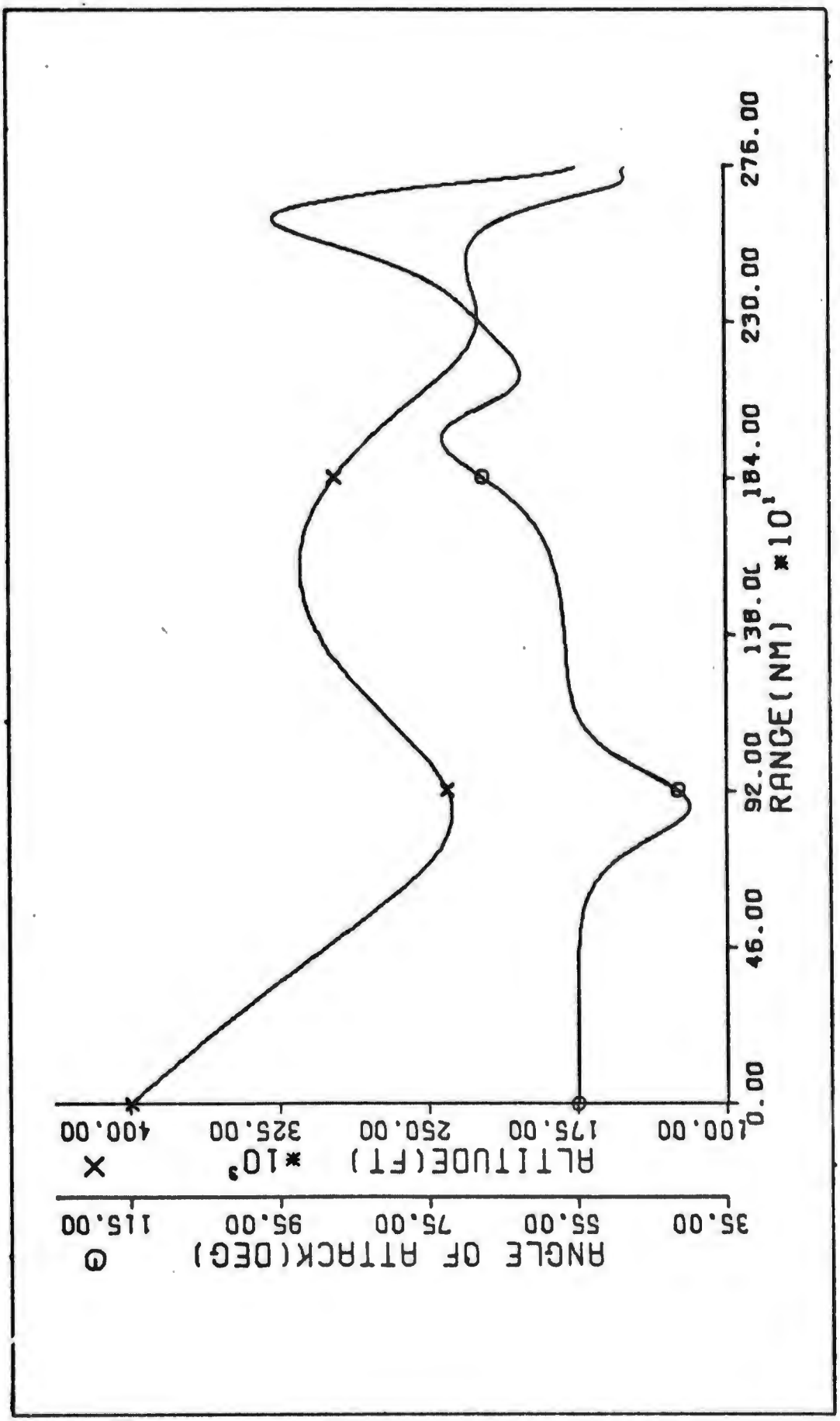

Figure 8. Control Schedule for Trajectory using Conjugate Gradient for 2755 nm Range

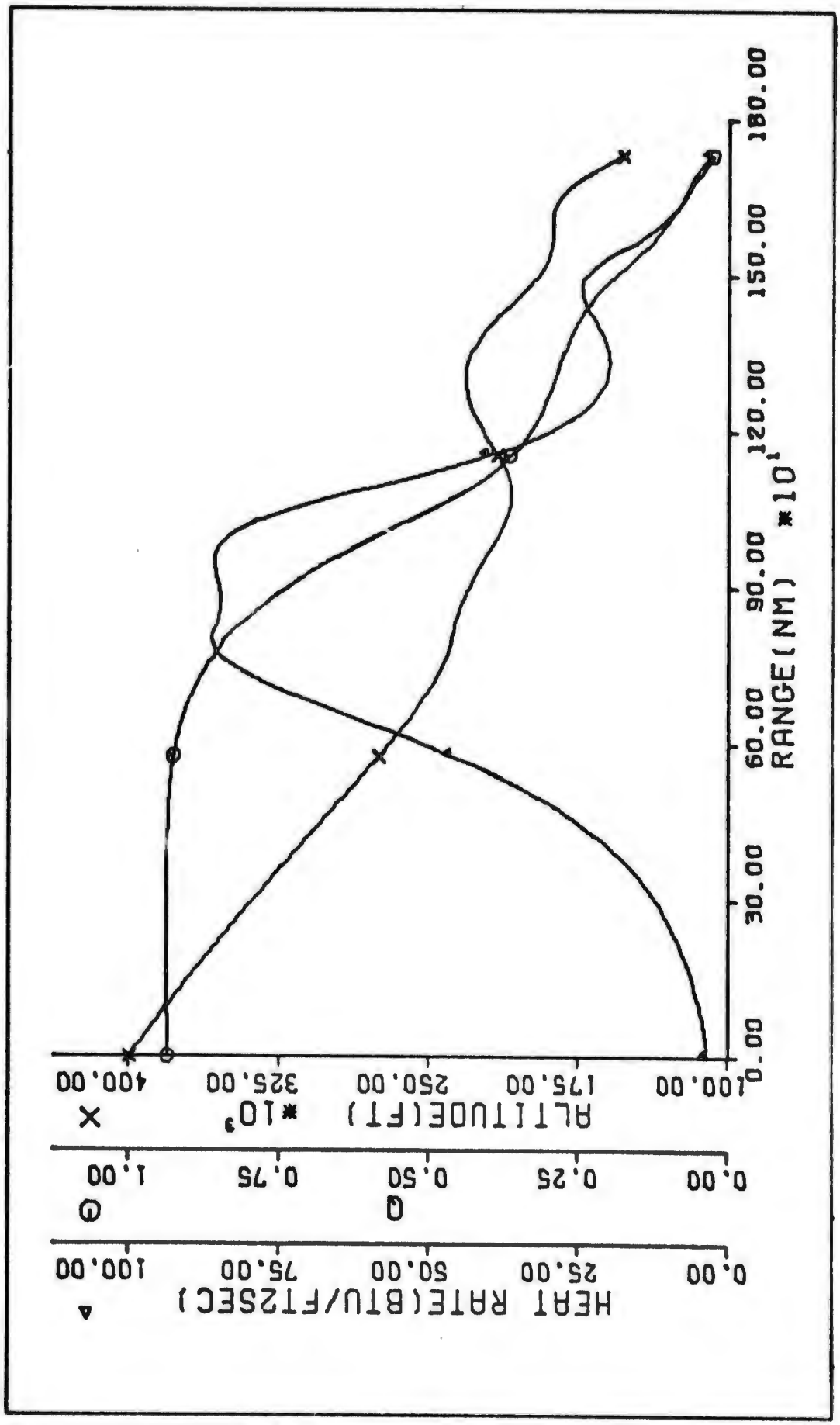

Figure 9. Reentry Trajectory using a Constant α up to the Peak Heating Rate then Conjugate Gradient for Total Range of 1730 nm

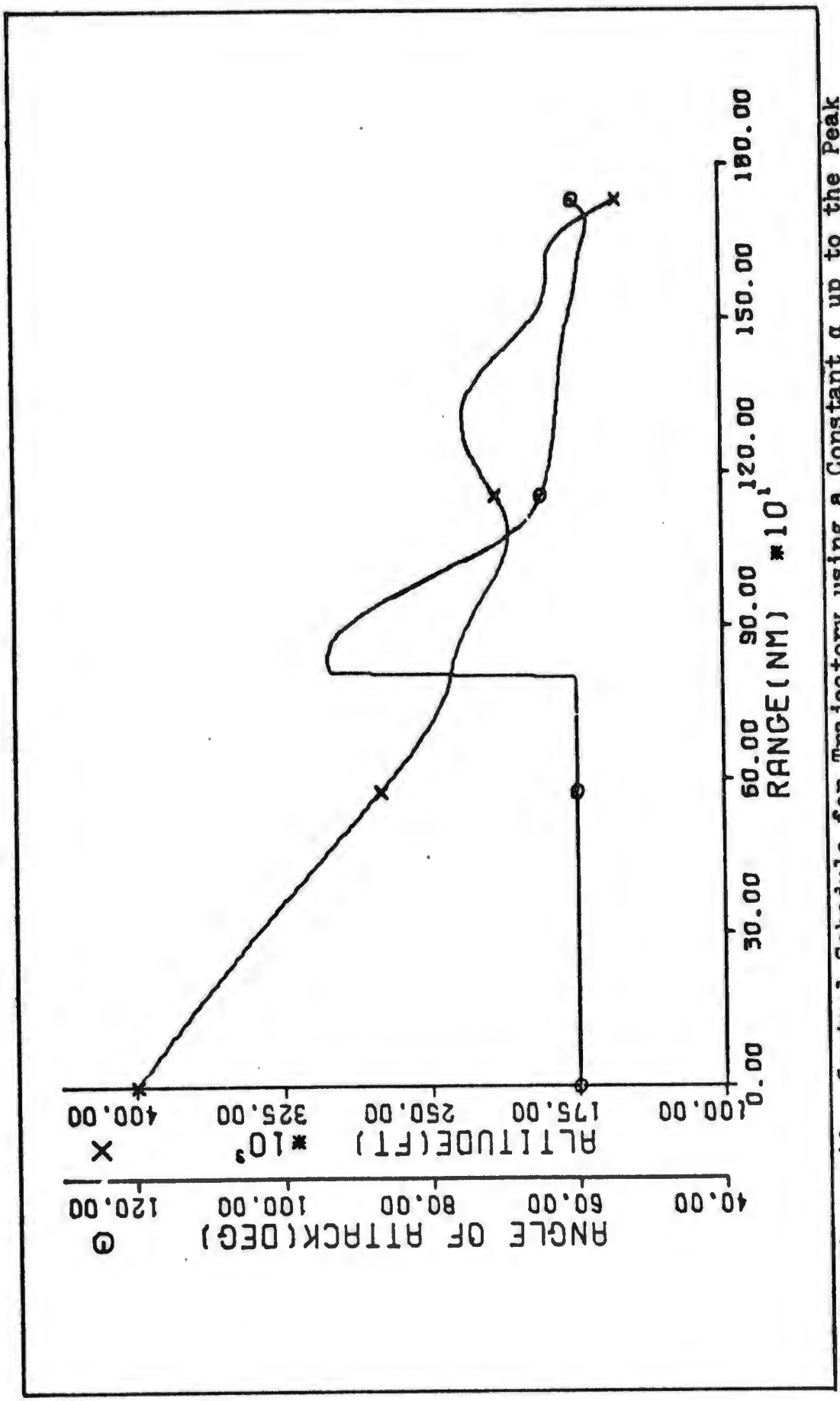

Figure 10. Control Schedule for Trajectory using a Constant α up to the Peak Heating Rate then Conjugate Gradient for Total Range of 1730 nm

TABLE I. REENTRY TRAJECTORIES USING CONJUGATE GRADIENT

(Initial conditions: h=399263 ft, v=24850 ft/sec, δ=1.7377°, Q=0.93557

Trajectory	Maximum Heat Rate (Btu/ft^2 sec)	Total Heat (Btu/ft^2)	Maximum Deceleration (g's)	Final Range (nm)	Final Altitude (ft)	Final Velocity (ft/sec)
Conjugate Gradient	94.5	19,380	3.49	1730	150,000	4000
Conjugate Gradient	90.3	29,364	6.3	2755	150,000	3109[a]
Constant α /Conj Grad	86.3	19,943	3.1	1730	150,000	4000

[a]Unconstrained

IV Q-Controller and Trajectories

With the reference trajectories of Chapter III developed, some correlation was sought between these trajectories and the resulting Q schedule. At first look, the Q curves seemed pretty well nondescript when taken as a whole. However, with three of the trajectories some correlation was found. In Figure 1, page 24, for the "equilibrium" glide trajectory, the plot for Q is nearly a straight line from about 750 nm to the final range. Also, in Figures 5, page 28, and 9, page 32, if a straight line is drawn from the initial to the final Q, the actual Q trajectory either approaches or oscillates about this straight line for approximately the last half of the trajectory. Another characteristic noted was that peaks in heating rate generally occurred where the slope of the Q trajectory was steepest. This was especially noticeable in Figures 3, 5, and 7 of Chapter III. It was then decided to try straightening the Q profile, or trajectory, such that the slope is controlled and possibly resulting in reduced peaks in the heating rate.

It should be noted that the cost function of the conjugate gradient optimization scheme was the integral of heating rate squared which is a compromise between minimizing the peak heating rate and the total heat, so the peaks in heating rate were not necessarily minimized. This

was shown to be the case in Chapter III where for one trajectory a constant angle of attack was used for part of the reentry trajectory, Figure 9. The peak heating rate was less in this case than in the case where the conjugate gradient technique was used for the whole trajectory, Figure 5. However, the conjugate gradient gave a lower total heat. It was not within the scope of this paper to ascertain which would be best but using the guidelines as they are i.e., peak heating rate below 100 Btu/ft^2 sec and total heat approaching that of an optimized trajectory, should be sufficient in assuring the structural integrity of the vehicle.

The Q-Controller

It was not known at the outset if straightening the Q profile was the best route to take but only a starting direction. To get a straight line Q trajectory, the first method attempted was using optimization techniques to track a desired Q trajectory. This was never successful as the control became saturated at points in the trajectory as there was not enough lift available to acheive the desired response. It was while attempting to find an optimization scheme to work that another alternative was sought and found.

Since it was a straight line that was desired end result, then dQ/dS desired was a constant. The state equation for dQ/dS, Equation 20, page 12, was solved for the control,

$$\alpha = \arcsin\left[\left\{\frac{\left[\frac{\tan\delta\,(2-Q)}{R_e} - \frac{dQ}{dS}\right] v^2 R_e \cos\delta}{\mu\, Q^2\, \rho\, (l^2/m)} - 0.042\right\} / 1.46\ \mathrm{sgn}\ \alpha\right]^{1/3} \tag{47}$$

It was this equation that allowed the proposed problem for this paper to be solved. At first glance it would seem that sgn α need by known before α can be determined. However, if α is constrained to be positive, this term can be ignored. This constraint does not limit the effectiveness of the control if the constraint is for α between 0° and 180°. The lift coefficient, drag coefficient and thus the lift-over-drag value for the mathematical vehicle model have the same meaning for α in the second quadrant as for α in the fourth quadrant and so any desired value for these terms can be reached within these limits for α. It was found that limiting α between 0° and 90° was sufficient.

All the parameters of this equation are either constants or states of the system except for dQ/dS, which will be referred to as the desired rate of change in Q with respect to range, $\dot{Q}_d$. With the equation set up in this manner, any trajectory for Q as a function of range can be followed if the trajectory has an explicit equation and that equation

has a derivative with respect to range-provided the vehicle model is controllable over this trajectory. That is, it is possible that Equation (47) would have no solution for part of the trajectory where the expression in brackets has a value greater than 1. Practically, this means the controller is asked to dissipate more energy (provide more drag) than is physically possible since the maximum is reached at $\alpha=90°$ or where $\sin\alpha=1$. The control is said to be "saturated" and the vehicle "uncontrollable" at these times, with α held at 90°. A control scheme which overcomes this possibility is presented in the next section.

Straight Line Q Trajectories

There are several ways to incorporate a straight line Q trajectory into the reentry problem. One is to try following a line from the initial Q at 399,263 ft altitude to the desired final Q, Q_{fd}. This is not practical, however, because at high altitudes the trajectory for reentry is nearly ballistic in nature and no value of control will force the vehicle to follow the proposed Q trajectory. As was brought out in the last chapter, a search was made for a constant angle of attack which minimized the peak heating rate for the specified initial conditions and was found to be 59.961 degrees. This control was then used for the initial part of the trajectory.

There are several logical points along the constant angle of attack trajectory where the straight line Q tra-

jectory could be initiated. The one selected for this study was where the peak heating rate occurred.

The desired final Q, Q_{fd}, was calculated using the desired final altitude, 150,000 ft, and a velocity of 4000 ft/sec which is midway between the range of velocities desired:

$$Q_{fd} = 0.023955591 \tag{48}$$

The desired rate of change in Q with respect to range, $\dot{Q}_d$, was calculated using

$$\dot{Q}_d = \frac{Q_{fd} - Q}{S_{tg}} \tag{49}$$

where Q was the current value of Q and S_{tg} was the range to go:

$$S_{tg} = S_f - S \tag{50}$$

where S_f was the desired final range from the initial entry point and S was the actual range obtained from the initial entry point. This value for $\dot{Q}_d$ was then inserted into Equation (47) and a control calculated. Some graphical examples of resulting trajectories are shown in Figures 11 and 13, and the control schedules for these trajectories are shown in Figures 12 and 14. Figures 11 and 12 are the results using a final range of 1730 nm and Figures 13 and 14 are results using a range of 2419 nm.

A distinct advantage in using this method for calculating $\dot{Q}_d$ is that it is continually being updated using the

current state of the system. So, even if the control limits of the vehicle model have been reached, eventually the vehicle returns to a controllable state and a new straight line Q trajectory is tracked. Of course, it is possible that the control becomes saturated toward the end of the trajectory and thus the vehicle model is unable to meet the desired end conditions. This does happen and is a limiting factor for the use of the Q-controller.

Table 1 shows the terminal conditions met by the vehicle model using various distances for the total surface range from entry. From the table a conservative estimate of the effective spread for this type of control scheme is 1900 nm, ranges 1550 through 3452 nm. With this estimate, the altitude would not be off by more than 9000 ft, or 6.0%, and velocity error would be negligible. The flight depression angle does have some spread but at the velocity being considered this could be readily changed in the transition phase of reentry. The peak heating rate for all the trajectories in this table was obtained while the constant angle of attack was still in affect, i.e., 86.28 Btu/ft^2 sec.

For all the trajectories considered within the range of the controller the highest deceleration force encountered was 2.13 g's. Therefore deceleration is not a limiting factor.

Table II shows the effects of changes in the initial condi:ions at entry on terminal conditions for a total

surface range of 2419 nm. The largest error in altitude from the desired 150,000 ft is 11,256 ft, 7.5%, for a spread in the initial velocities of 1600 ft/sec, ± 3.2%. Further examination of the table shows that even for desired initial conditions the altitude is off by 6563 ft, 3.3%. However, for all trajectories the errors in the terminal velocities are negligible. Variations in the initial flight depression angle have a similar effect on altitude. The largest error in altitude is 7371 ft, 4.9%, for a spread in initial δ of 0.34 degrees, ± 9.8%. Variations in the terminal flight depression angle were not significant for the perturbations considered though no direct consideration was given to this parameter in the controller.

Maximum deceleration for any perturbed trajectory for this range was less than 2 g's and again was not considered a limiting factor.

Whether the variations in these end results are acceptable initial conditions for the transition phase of reentry depends a great deal on the scheme used for that phase. Reference 7 considered perturbations of 100 ft/sec, 1°, and 1000 ft in velocity, flight depression, and altitude respectively. While the variations in h and δ for the Q controlled reentry is greater than those of Reference 7, there is enough energy lift in the system that these variations could be absorbed.

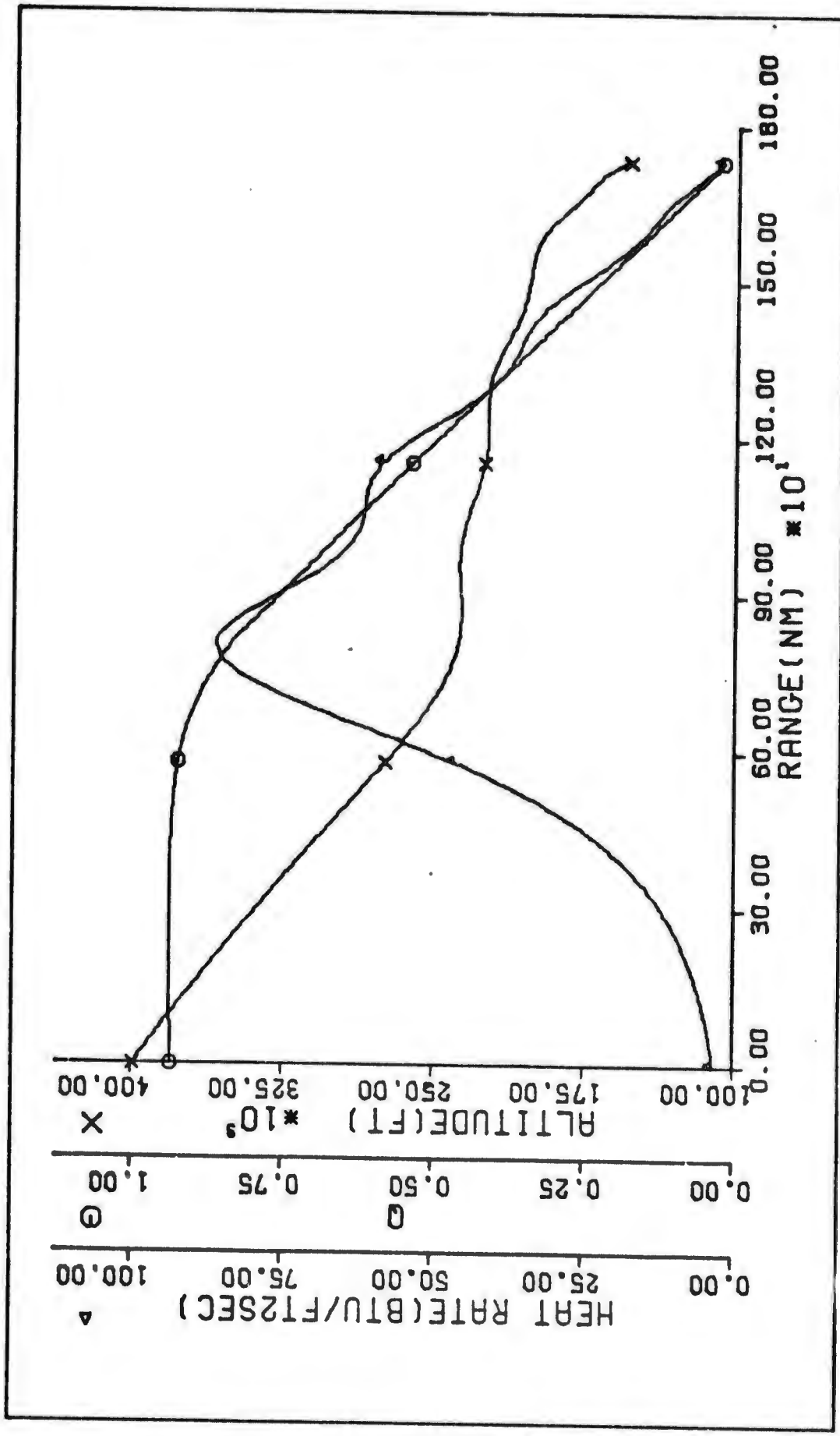

Figure 11. Reentry Trajectory using the Straight Line Q-Controller over 1730 nm Total Range

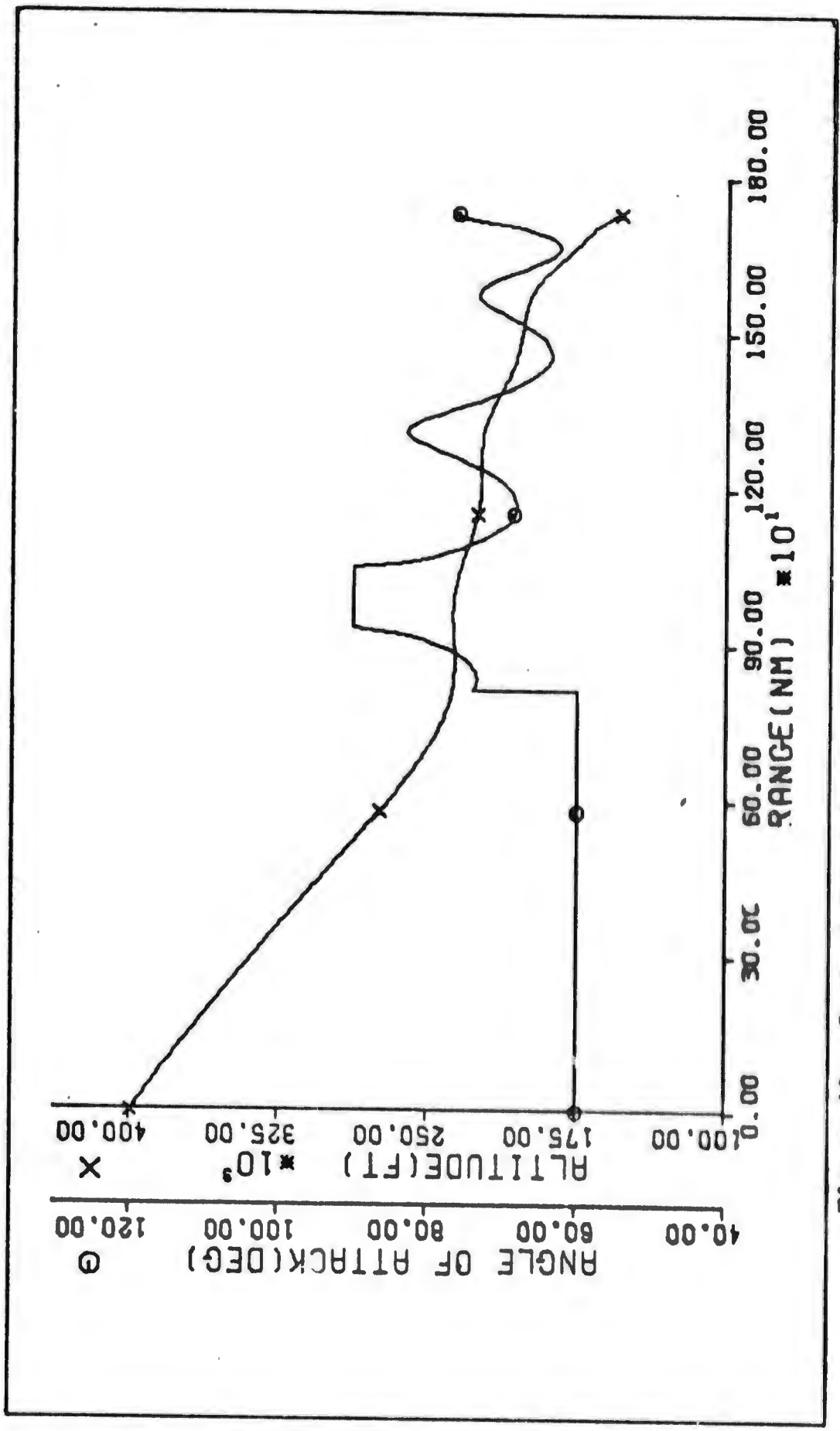

Figure 12. Control Schedule for Trajectory using the Straight Line Q-Controller over 1730 nm Total Range

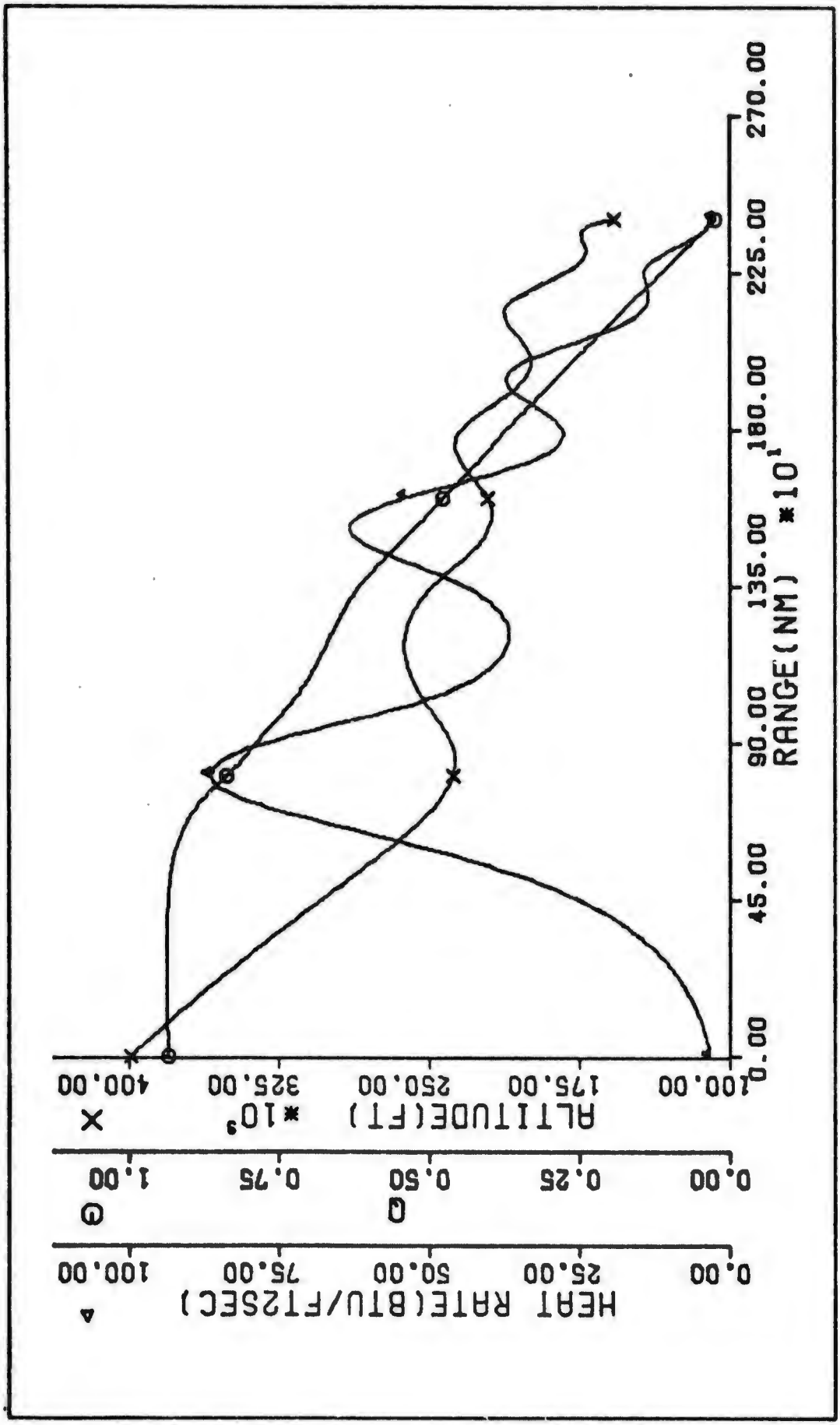

Figure 13. Reentry Trajectory using the Straight Line Q-Controller over 2419 nm Total Range

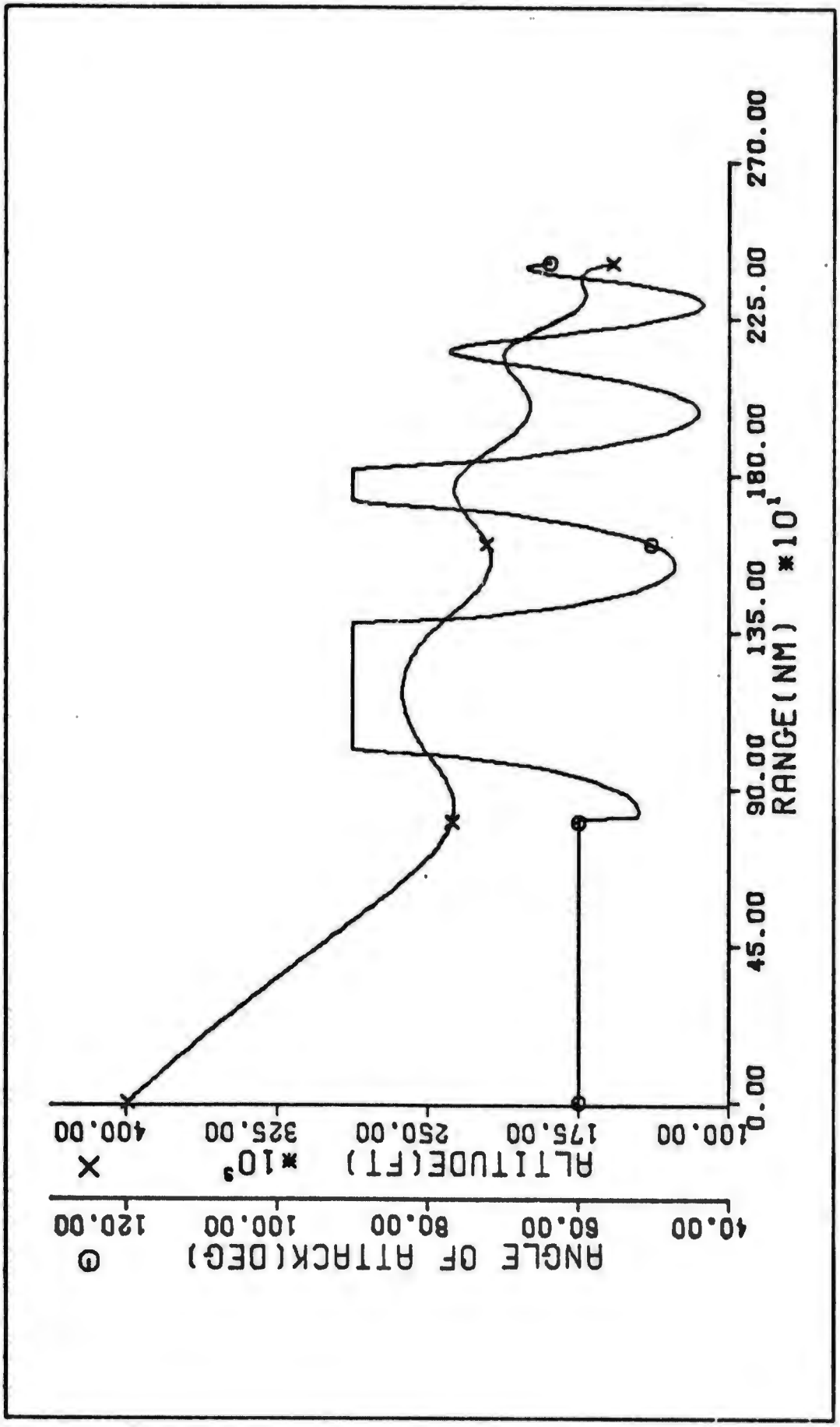

Figure 14. Control Schedule for Trajectory using the Straight Line Q-Controller over 2419 nm Total Range

TABLE II. TERMINAL CONDITIONS OF STRAIGHT LINE Q TRAJECTORIES FOR DIFFERENT SURFACE RANGES[a]

(Initial conditions: h=399263 ft, v=24850 ft/sec, δ=1.7377°, Q=0.93557
Desired terminal conditions: h=150,000 ft, v=4000 ft/sec, Q=0.02395559)

Surface Range (nm)	Surface Range (Du)[b]	Q_f	Velocity (ft/sec)	Altitude (ft)	Flight Depression Angle (deg)	Total Heat (Btu/ft^2)
1378	0.4000	.02401882	4006.1	141296	10.895	17407
1550	0.4500	.02395561	4000.2	147972	8.806	18955
1722	0.5000	.02395561	3999.7	153575	8.137	20621
1730	0.5025	.02395561	3999.6	153838	8.018	20719
2074	0.6000	.02395561	3999.1	158994	5.889	24506
2419	0.7000	.02395569	3999.4	156563	8.126	28308
2763	0.8000	.02395563	4000.4	146043	5.634	32344
3108	0.9000	.02395558	4000.7	142596	1.810	36849
3452	1.0000	.02395559	4000.7	143100	1.311	42020
3796	1.1000	.02395560	4001.1	137998	1.705	48084
4141	1.2000	.02395563	4003.0	118441	2.506	55905

[a]All trajectories had the same peak heat rate of 86.28 Btu/ft^2 sec

[b]1Du = 3443.934 nm (radius of earth) or 1Du = 1 radian (angular measurement of range)

TABLE III. EFFECTS OF PERTURBATIONS IN INITIAL CONDITIONS ON TERMINAL CONDITIONS[a]

(Straight line Q trajectories over a fixed range of 2419 nautical miles, fixed initial altitude of 399263 feet)

Initial Conditions		Terminal Conditions		
Velocity, v (ft/sec)	Flt. Depression Angle, δ (deg)	Altitude, h (ft)	Velocity, v (ft/sec)	Flt. Depression Angle, δ (deg)
24850	1.73778	156563	3999.4	8.126
24050	"	161256	3998.9	6.358
24450	"	159949	3999.1	7.707
25250	"	150856	3999.9	6.364
25650	"	154679	3999.6	5.005
24850	1.56778	155360	3999.5	7.685
"	1.65278	155998	3999.4	7.924
"	1.82278	157031	3999.3	8.335
"	1.90778	157371	3999.3	8.576

[a]Desired terminal conditions: h=150000 ft, v=4000 ft/sec

Second Order Q Trajectories

Another type of trajectory given consideration was one which more closely approximates the optimal of Figures 5, (page 28) and 9 (page 32). Again drawing a straight line from the initial Q to Q_{fd}, the actual Q trajectory approaches this line very nearly as a second order system would with the straight line as the input. Figure 15 shows these two curves and defines a few points on these curves that helped derive the equation for the second order approximation.

Subtracting Q from Q_d results in a second order system starting at point Q_o' with some initial negative value, a slope equal to zero, and an input equal to zero. This is shown in Figure 16.

Noting that

$$Q_d = Q_o + \dot{Q}_d S \tag{51}$$

and

$$\Delta Q = Q_d - Q \tag{52}$$

then

$$\frac{d}{dS} \Delta Q = \frac{d}{dS} (Q_o + \dot{Q}_d S - Q)$$

$$= \dot{Q}_d - \dot{Q} \tag{53}$$

therefore

$$\dot{Q} = \dot{Q}_d - \Delta\dot{Q} \tag{54}$$

where $\Delta\dot{Q}$ is the derivative of ΔQ with respect to range.

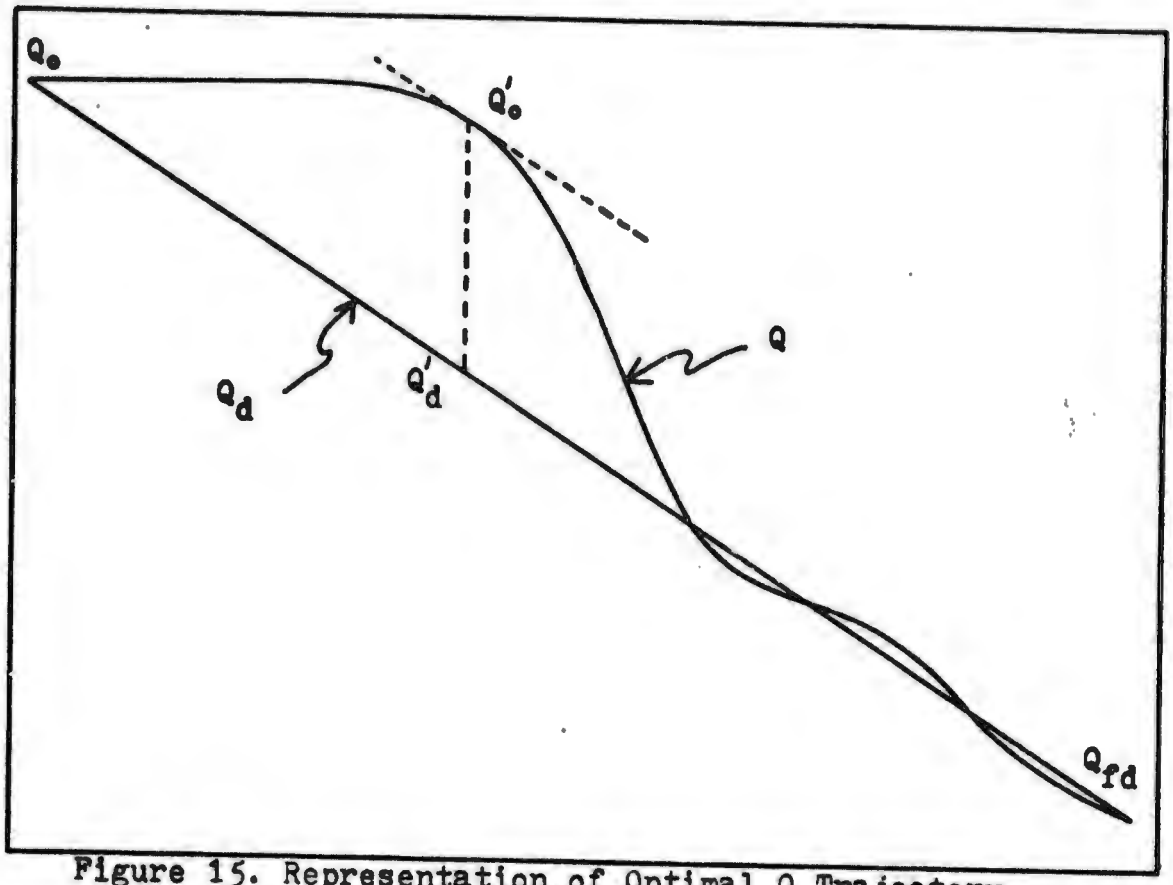

Figure 15. Representation of Optimal Q Trajectory over 1730 nm Total Range as it Approaches a Straight Line

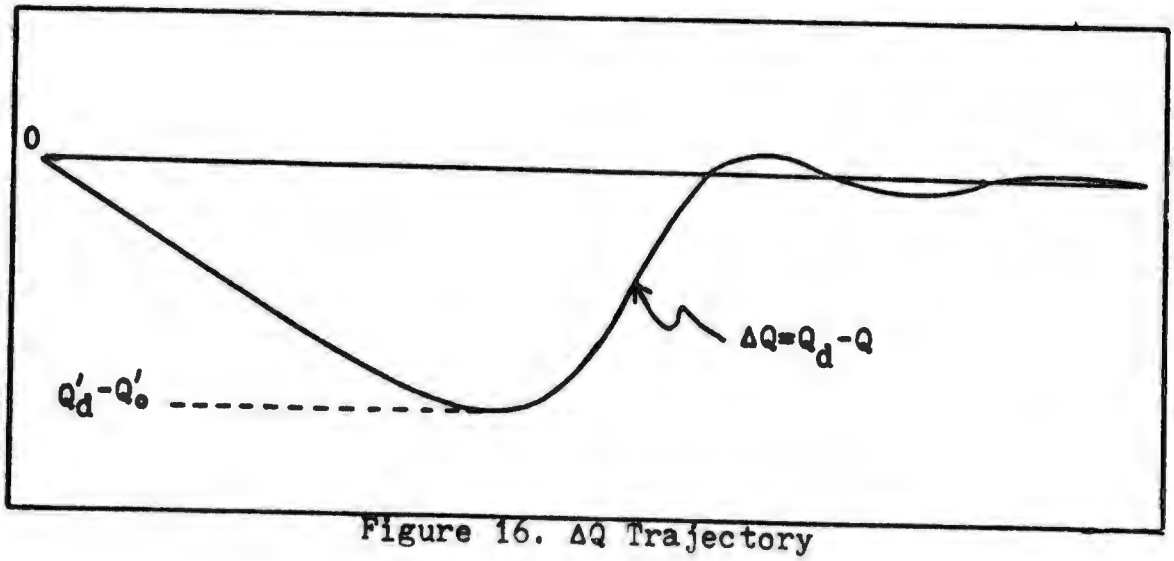

Figure 16. ΔQ Trajectory

It was then assumed that the curve, ΔQ, of Figure 16 was the result of a second order equation starting at a point along the actual Q trajectory where the slope of the actual Q trajectory equaled that of the desired Q. Then,

$$\ddot{\Delta Q} + 2\zeta\omega_n \dot{\Delta Q} + \omega_n^2 \Delta Q = 0 \tag{55}$$

where, as stated before, the input is zero and the initial condition for ΔQ is $Q'_d - Q'_o$. Then the steady state solution for Equation (55) is zero.

The general transient solution is (Ref 6)

$$\Delta Q = Ae^{-\zeta\omega_n S'} \sin\left(\omega_n\sqrt{1-\zeta^2}\, S' + \varpi\right) \tag{56}$$

and

$$\dot{\Delta Q} = -\zeta\omega_n Ae^{-\zeta\omega_n S'} \sin\left(\omega_n\sqrt{1-\zeta^2}\, S' + \varpi\right)$$

$$+\omega_n\sqrt{1-\zeta^2}\, Ae^{-\zeta\omega_n S'} \cos\left(\omega_n\sqrt{1-\zeta^2}\, S' + \varpi\right) \tag{57}$$

where S' is a surface range initialized at 0 beginning at that point where Q equals Q'_o. Using the initial conditions for ΔQ and $\dot{\Delta Q}$, Equation (56) becomes

$$Q'_d - Q'_o = A \sin \varpi \tag{58}$$

and Equation (57) becomes

$$0 = -\zeta \sin \varphi + \sqrt{1-\zeta^2} \cos \varphi \tag{59}$$

It can be shown from these equations that

$$\varphi = \arccos \zeta \tag{60}$$

Also, the time constant (Ref 6)

$$T = \frac{1}{\zeta \omega_n} \tag{61}$$

The number of time constants from the start of the guidance scheme to the final range can be adjusted by

$$nT = S_{tg} \tag{62}$$

where n is the parameter used to adjust the number of time constants and S_{tg} is the range to go from the start of the guidance scheme. For a given n and ζ all the constants for Equation (57) are known:

$$\omega_n = \frac{n}{\zeta S_{tg}} \tag{63}$$

$$\varphi = \arccos \zeta \tag{60}$$

and

$$A = \frac{Q'_d - Q'_\bullet}{\sin \varphi} \tag{64}$$

Therefore $\Delta\dot{Q}$ is known as a function of range for the remainder of the flight and since $\dot{Q}_d$ is a known constant a desired rate of change with respect to range of the actual Q, $\dot{Q}$, can be found using Equation (54). This $\dot{Q}$ was then used in Equation (47), page 37, to calculate α.

An example trajectory is shown graphically in Figure 17 and the control schedule in Figure 18. For this example ζ was 0.7 and n was 3. Other values were also used but these gave the best results. This trajectory had the lowest peak heat rate of any of those tried, 85.87 Btu/ft^2 sec. However, this was only 0.41 Btu/ft^2 sec less than was obtained using the constant α of 59.961° and the terminal values were further off than for any other control scheme. The reason for the terminal values being so far from the desired conditions is because the control scheme is completely specified at initiation and therefore if the vehicle model is unable to track the specified Q trajectory there is no way for the control scheme to correct for the error. The terminal values for altitude and velocity were 143926 ft and 3296 ft/sec respectively.

Table IV gives a comparison of the different trajectories resulting from the control schemes used in this paper for a total surface range of 1730 nm. From this table can be seen that the use of optimization schemes resulted in

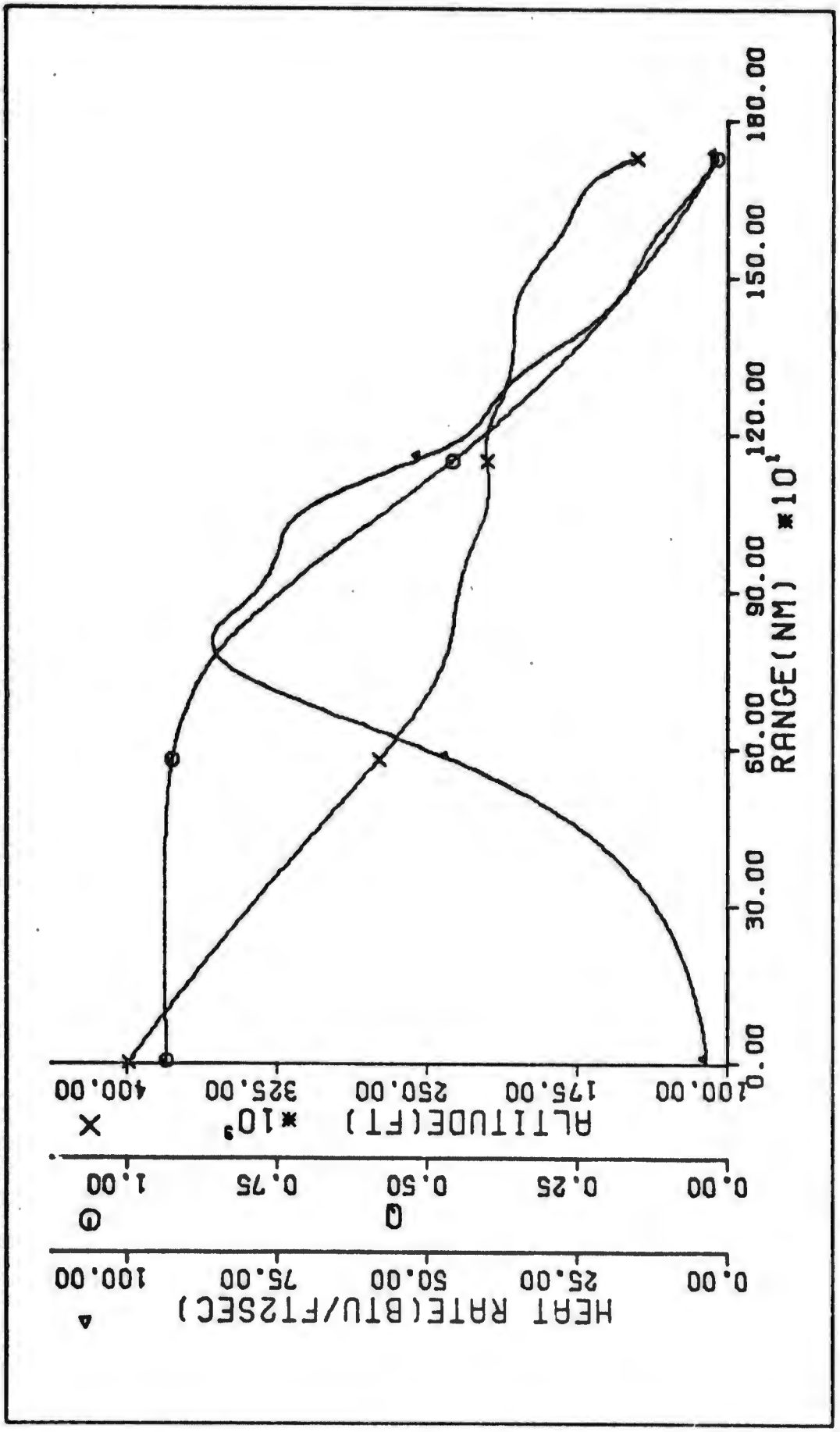

Figure 17. Reentry Trajectory using Second Order Approximation to Optimal over 1730 nm Total Range

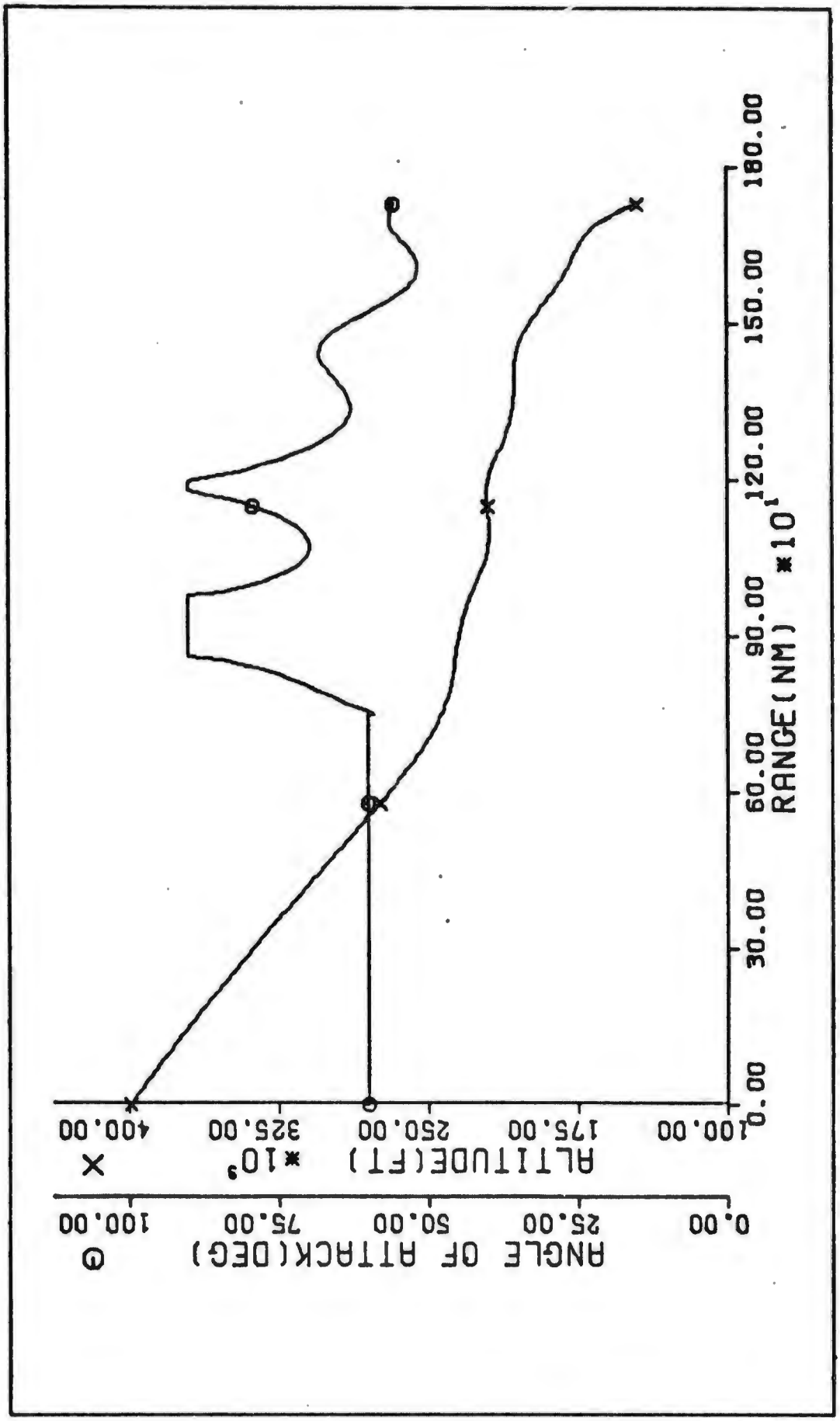

Figure 18. Control Schedule from Trajectory using Second Order Approximation to Optimal over 1730 nm Total Range

meeting the desired end conditions and lower total heat absorbed. The straight line Q controller met the final end conditions fairly well but had the highest total heat. However, the straight line Q trajectory has a low peak heat rate which could offset the higher total heat and has inherent self-correcting features and simplicity which would be desirable for an onboard controller. The second order controller also has the advantage of simplicity but, referring to Figure 7 of Chapter III, its usefulness over any sizeable range difference is questionable, besides not being able to meet end conditions.

TABLE IV. COMPARISON OF CONTROL SCHEMES USED

(Initial conditions: h=399263 ft, v=24850 ft/sec, δ=1.73778°, total range = 1730 nm)

Control Scheme	Final Altitude (ft)	Final Velocity (ft/sec)	Peak Heat Rate (Btu/ft^2 sec)	Total Heat (Btu/ft^2)
Conjugate Gradient	150000	4000.0	94.54	19380
[a]Constant α/ Conj. Grad.	150000	4000.0	86.28	19943
Constant α/ Strt. Line Q	153838	3999.6	86.28	20719
Constant α/ 2nd Order Q	143926	3296.0	85.87	20228

[a]Angle of attack, α = 59.961°

V Conclusions and Recommendations

Conclusions

From the results of this study it can be concluded that the nondimensional ballistic parameter Q does lead to a feasible control scheme for atmospheric reentry. The straight line Q controller developed in this paper meets all the criteria for a desirable controller except the meeting of the exact desired end condition on altitude. However, with the energy left in the system this could be compensated for in the transition phase for reentry. The fact that the control scheme meets all the other terms in the criteria shows it has merit. The scheme meets the criteria on heating rate, total heat, deceleration and on obtaining a desired final velocity. It is flexible in that it has the capability of updating itself continually as the system's become better known, or if the vehicle should become uncontrollable, in the sense that the control is saturated, for a part of the reentry trajectory. The scheme will pick up again when the vehicle returns to a controllable state. Also the computational aspects are simple enough for onboard calculation of control with a minimum in storage requirements for data. The control scheme also works over a wide spread of total surface range.

Recommendations

There were several aspects that were not covered in this investigation and development that may be worthwhile looking into. One would be the investigation of transition phase guidance schemes that would be able to handle the variations in initial conditions generated in the Q controlled trajectories. It is possible that a more judicious choice in the desired final Q would lead to more consistent end conditions. These final Q values may be a function of the total surface range to be covered, initial velocity, or even the initial flight depression angle. Adding such conditions may complicate the control scheme somewhat but if the end result is more consistency the extra computation would be worth it.

Finally, since this study was a preliminary feasibility study, it was done using only two dimensional equations of motion. The control scheme would have to be extended to full six-degree-of-freedom equations before its full worth can be ascertained.

Bibliography

1. Bate, R.R., et al. Fundamentals of Astrodynamics. New York: Dover Publications, Inc. 1971.

2. Brown, F.M., et al. Guidance and Control Theory with Applications to Aerospace Vehicles. AFLC WPAFB May 70 250. Wright-Patterson AFB, Ohio: Lecture Series, June 1970.

3. Duncan, R.C., Dynamics of Atmospheric Entry. New York: McGraw-Hill Book Co., 1962.

4. Lasdon, L.S., et al. "The Conjugate Gradient Method for Optimal Control Problems." IEEE Transactions on Automatic Control, AC-12, NO. 2: 132-138 (April 1967).

5. Wrigley, W., et al. Gyroscopic Theory, Design, and Instrumentation. Cambridge, Mass.: The M.I.T. Press, 1969.

6. D'Azzo, J.J. and Houpis, C.H., Feedback Control System Analysis and Synthesis. New York: McGraw-Hill Book Co., 1966.

7. Stengel, R.F., "Optimal Transition from Entry to Cruising Flight." Journal of Spacecraft and Rockets, 8-11: 1126-1132 (November 1971).

8. Bryson, A.E., Denham, W.F., "A Steepest-Ascent Method for Solving Optimum Programming Problems." Journal of Applied Mechanics, 29-E2: 247-257 (June 1962).

9. South, D.J., An Analysis of Real-Time Optimal Guidance of Lifting Re-entry Vehicles. Unpublished doctoral dissertation. Wright-Patterson AFB, Ohio: Air Force Institute of Technology, August 1973.

APPENDIX A

Derivation of Equations of Motion

Before applying the theorem of Coriolis to derive the state equations, a system of coordinate frames is first defined. In Figure 19 is illustrated the relationship between the three coordinate frames used in deriving the state equations. The E-frame is a locally inertial frame which is fixed to an assumed non-rotating earth at the start of the reentry problem. The N-frame is the earth centered navigation frame which rotates about the center of the earth with the movement of the vehicle. The B-frame is the velocity frame and fixed relative to the vehicles velocity vector.

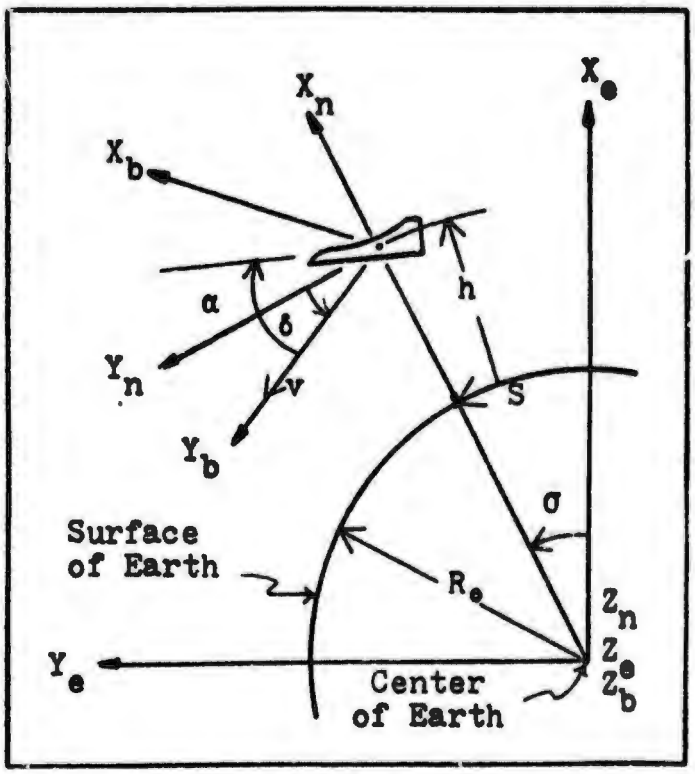

Figure 19.
Coordinate Systems E, N, and B

From the theorm of Coriolis (Ref 5) the acceleration of the vehicle (considered a point mass) with respect to the E-frame and expressed in N coordinates is

$$\ddot{\underline{R}}_e\Big|_n = \ddot{\underline{R}}_n + 2\omega_{en} \times \dot{\underline{R}}_n + \dot{\omega}_{en} \times R_n + \omega_{en} \times (\omega_{en} \times R_n) \tag{65}$$

where R is the sum of the radius of the earth, R_e, and the altitude of the vehicle, h. The subscripts for R indicate the frame the $\underline{R}$ vector is in. The rate of angular rotation of the N-frame with respect to the E-frame is given by ω_{en}. By inspection

$$\omega_{en} = \begin{bmatrix} 0 \\ 0 \\ \frac{v \cos \delta}{R} \end{bmatrix}_N \tag{66}$$

where the subscript N indicates the vector is in the N-frame. v is the velocity of the vehicle in the velocity frame and δ is the flight depression angle. The flight depression angle is positive as shown in Figure 19 and defined as the angle between the local horizontal, y-axis of the N-frame, and the velocity vector of the vehicle, y axis of the B-frame. Taking the time derivative of the Z component of the ω_{en} vector

$$\dot{\omega}_{en}\ \bar{Z}_n = \frac{R(\dot{v} \cos \delta - v\dot{\delta} \sin \delta) - \dot{R}v \cos \delta}{R^2}\ \bar{Z}_n \tag{67}$$

$\bar{Z}_n$ is the unit vector in the Z direction of the N-frame. Henceforth, all unit vectors will be denoted in the same manner.

The instantaneous rate of change of the radius vector with respect to the N-frame

$$\dot{\bar{R}}_n = \begin{bmatrix} -v \sin \delta \\ 0 \\ 0 \end{bmatrix}_N \tag{68}$$

Acceleration with respect to the N-frame, is then

$$\ddot{\bar{R}}_n \bar{x}_n = (-\dot{v} \sin \delta - v\dot{\delta} \cos \delta)\bar{x}_n \tag{69}$$

The appropriate cross products are now taken and summed

$$\ddot{\bar{R}}_e\Big|_N = \begin{bmatrix} -\dot{v} \sin \delta - v\dot{\delta} \cos \delta - v^2 \cos^2 \delta / R \\ R(\dot{v} \cos \delta - v\dot{\delta} \sin \delta) - \dot{R}v \cos \delta - \dfrac{2v^2 \cos \delta \sin \delta}{R} \\ 0 \end{bmatrix} \tag{70}$$

It is desired to have velocity frame coordinates for on board computation. The coordinate transformation matrix (Ref 5) from N coordinates to B coordinates is

$$C_B^N = \begin{bmatrix} \cos \delta & \sin \delta & 0 \\ -\sin \delta & \cos \delta & 0 \\ 0 & 0 & 1 \end{bmatrix} \tag{71}$$

After premultiplying $\ddot{\bar{R}}_e\Big|_N$ by C_B^N and simplifying

$$\ddot{\bar{R}}_e\Big|_B = \begin{bmatrix} -v\dot{\delta} - v^2 \cos\delta/R \\ \dot{v} \\ o \end{bmatrix} \tag{72}$$

Using Newton's second law of motion, the acceleration can be equated to the specific forces acting on the vehicle. The forces acting on an unpowered reentry lifting body are lift, drag and gravity. Lift is perpendicular to the velocity vector, the x_b direction, and drag is opposite of the velocity vector, $-y_b$ direction. Using two body mechanics and the fact that the mass of the earth is much greater than that of the vehicle, the force acting on the vehicle due to gravity is

$$\bar{F}_g = -\frac{GM}{R^3}\,\bar{x}_n \tag{73}$$

where G is the universal gravitational constant and M is the mass of the earth. The coordinate transformation into the B-frame is applied to this force and the earth's gravitational parameter, $\mu = GM$, is used. The forces are summed and then equated to the acceleration:

$$\begin{bmatrix} -v\dot{\delta} - v^2 \cos\delta/R \\ \dot{v} \\ o \end{bmatrix} = \begin{bmatrix} L - \frac{\mu}{R^3}\cos\delta \\ -D + \mu/R^3 \sin\delta \\ o \end{bmatrix} \tag{74}$$

Solving for $\dot{\delta}$ and $\dot{v}$

$$\dot{\delta} = \frac{-v^2 \cos \delta}{Rv} + \frac{\mu \cos \delta}{R^3 v} - \frac{L}{v} \tag{75}$$

and

$$\dot{v} = \frac{\mu \sin \delta}{R^3} - D \tag{76}$$

where L is the specific lift of the vehicle and D is the specific drag. Using these equations and two others which were defined during the derivation, those for $\dot{R}_b$ and ω_{en}, the resulting state equations are

$$\dot{\delta} = \frac{-v^2 \cos \delta}{Rv} + \frac{\mu \cos \delta}{R^3 v} - \frac{L}{v} \tag{77}$$

$$\dot{v} = \frac{\mu \sin \delta}{R^3} - D \tag{78}$$

$$\dot{R} = - v \sin \delta \tag{79}$$

$$\dot{\sigma} = \omega_{en} = \frac{v \cos \delta}{R} \tag{80}$$

where σ is the angle between the inertial earth centered frame and the navigational frame. This is the range angle and can be converted to the surface range by multiplying by the radius of the earth, R_e. Also $\dot{R}$ can be replaced with $\dot{h}$ since $R = R_e + h$ and R_e is assumed to be a constant.

APPENDIX B

Conjugate Gradient

The algorithm for the conjugate gradient optimization technique used in this paper to generate nominal reentry trajectories was taken from a paper by L.S. Lasdon, S.K. Mitter, and A.D. Waren (Ref 4). The algorithm uses penalty functions to convert constrained optimal control problems to unconstrained problems. It requires more storage than the steepest descent method in that beside the gradient trajectory being stored, the norm squared of the gradient and the actual direction of search must also be stored. However, the number of iterations necessary for convergence to a local minimum is much less for the conjugate gradient.

Problem Formulation

The problem formulation used in reference 4 is based on a cost function being in Meyer form, i.e., a function of the states evaluated at the final value of the independent variable. Using t to represent the independent variable, the cost function is

$$J = \varphi(\underline{x}(t_f)) \tag{81}$$

where $\underline{x}$ is an n vector. If the desired cost function is of integral form, a new state can be defined such that its derivative is the integrand of the cost function and a new cost

function in Meyer form results. Any terminal constraints can then be added as penalty functions. Initial conditions have to be known, and as implied in the above discussion, the initial and final values of the independent variable have to be known. Then the general formulation of the optimization problem is

$$\text{minimize} \quad J = \Phi(\underline{x}(t_f)) \tag{82}$$

$$\text{subject to} \quad \dot{\underline{x}} = \underline{f}(\underline{x},\underline{u},t) \tag{83}$$

$$\text{given that} \quad \underline{x}(t_o) = \underline{c} \tag{84}$$

where $\underline{x}$ is an n vector, u is an m vector, t_o is the initial value of the independent variable and t_f is its final value, and both t_o and t_f are known.

The Hamilton, for the Meyer form of the cost function, is

$$H = \sum_{i=1}^{m} \lambda_i f_i \tag{85}$$

where the costate vector, λ, is an n vector and

$$\dot{\lambda}_i = - \sum_{j=1}^{n} \lambda_j \frac{\partial f_j}{\partial x_i} \tag{86}$$

The values for the costates at t_f are

$$\lambda_i(t_f) = \left. \frac{\partial \Phi}{\partial x_i} \right|_{t=t_f} \qquad i=1,2,\ldots,n \tag{87}$$

the gradient is

$$\underline{g}(\underline{u}) = \frac{\partial H}{\partial \underline{u}} \tag{88}$$

and $\underline{g}(\underline{u})$ is an m vector. Up to this point the formulation is the same as for a steepest descent technique. In fact, the conjugate gradient technique does use the negative direction of the gradient for its first search direction but in subsequent iterations the direction is altered by the ratio of the current to the previous norms squared of the gradient and the previous search direction.

Algorithm

The algorithm for the case where there is only one control variable, m = 1, proceeds as follows:

1. An arbitrary initial control trajectory, u_o, is chosen and stored.

2. The state equations are integrated forward using u_o. The costates are evaluated at t_f and integrated backward using u_o. Both the state and costate trajectories are stored.

3. The gradient trajectory g_o is calculated using the values obtained in (1) and (2) and the initial search direction, s_o, is set equal to the negative of g_o.

4. A one dimensional search is made for an α which minimizes the cost function which is now a function of the previous control trajectory plus α times

the search direction. That is

$$\alpha = \alpha_i \text{ which minimizes } J(u_i + \alpha s_i) \tag{89}$$

where i refers to the iteration number starting with o. The states are integrated forward using $u = u_i + \alpha s_i$ to evaluate J.

5. With an α found, a new control trajectory is calculated and stored

$$u_{i+1} = u_i + \alpha s_i \tag{90}$$

6. The states are integrated forward using the new control, u_{i+1}, and stored. If the desired stopping condition is reached, a nominal state trajectory has been reached. (The stopping condition used in the computer program for this paper was that the cost function did not change more than a specified value.)

7. If the stopping condition has not been met, the costates are evaluated at t_f, integrated backwards, and stored.

8. The norm squared of the gradient is calculated by integrating the stored gradient squared, i.e.

$$(g_i, g_i) = \int_{t_o}^{t_f} g_i(t) g_i(t) dt \tag{91}$$

(Rectangular approximations were used in the computer program for this paper.) Then a new gradient, g_{i+1}, is calculated using the results of (6) and (7). This is stored and its square

is integrated. A ratio, β_i, is given by

$$\beta_i = (g_{i+1}, g_{i+1}) / (g_i, g_i) \tag{92}$$

where (g, g) is as defined above.

9. The new search direction is given as

$$s_{i+1} = - g_{i+1} + \beta_i s_i \tag{93}$$

this trajectory is stored and the algorithm continues at step (4).

Vita

Dennis Navin was born on 12 May 1942 in Jackson, Mississippi. He graduated from St. Gregory's High School, Shawnee, Oklahoma in May 1960 and enlisted in the Air Force in September 1961. After technical training at Lowry AFB, Colorado, he was assigned as a Gunnery Trainer Specialist at Bergstrom AFB, Texas, where he cross-trained to ECM Trainer Specialist. While stationed at March AFB, California, he entered the Airmen Education and Commissioning Program. He received a Bachelor Degree in Electrical Engineering from Sacramento State College, in Sacramento, California, in June, 1971. He received his commission as a Second Lieutenant in the U.S. Air Force in September, 1971. His first duty assignment as an officer was to the Air Force Institute of Technology, as a Master's Degree Student.

Permanent address: 802 N Pottenger
Sha[illegible]e [illegible]klahoma

This thesis was typed by Mrs. Sheila Navin